GJO–2003–495–TAC

Pinellas Environmental Restoration Project

Simulation of Enhanced Bioremediation at the Building 100 Area

October 2003

U.S. Department of Energy

Work Performed Under DOE Contract No. DE–AC13–02GJ79491 for the U.S. Department of Energy, Grand Junction, Colorado.
Approved for public release; distribution is unlimited.

GJO−2003−495−TAC
PIN 700.20.10

Pinellas Environmental Restoration Project

Young - Rainey STAR Center

Simulation of Enhanced Bioremediation at the Building 100 Area

October 2003

Prepared by
U.S. Department of Energy
Grand Junction, Colorado

Work Performed Under DOE Contract Number DE–AC13−02GJ79491

N0064700

Contents

1.0 Introduction 1
2.0 Assessment of HRC Penetration 1
2.1 Penetration Radius Based on Volume 2
2.2 Penetration Radius Based on Transport 2
2.2.1 HRC Injection For Various Durations 3
2.2.2 Radial Transport Summary 3
3.0 Lactic Acid Migration 4
3.1 Diffusion of Lactic Acid 4
3.1.1 Relative Concentration 4
3.1.2 Estimated Lactic Acid Diffusion Coefficient 7
3.2 Conclusions 8
4.0 Pilot Test Study Modeling 8
4.1 Combined Advective-Dispersive Transport of Lactic Acid 9
4.2 Diffusion Coefficient Sensitivity Analysis 14
4.3 Full Scale Barrier Wall Design 15
4.4 Conclusions 16
5.0 MT3DMS Basic Advective-Dispersive Modeling 18
5.1 Diffusion Coefficient = 0.2 ft^2/day 19
5.1.1 Component 1—Vinyl Chloride 19
5.1.2 Component 2—Organic Acid 21
5.1.3 Porosity and Half-life Sensitivity 24
5.2 Diffusion Coefficient = 0.002 ft^2/day 25
5.2.1 Component 1—Vinyl Chloride 25
5.2.2 Component 2—Organic Acid 27
5.2.3 Porosity and Half-life Sensitivity 31
5.3 Diffusion Coefficient Sensitivity 31
5.4 MT3DMS Model Conclusions 32
6.0 RT3D Modeling 33
6.1 Stoichiometric Ratio F = 10 33
6.2 Stoichiometric Ratio F = 10000 37
6.3 Stoichiometric Ratio Sensitivity 40
6.4 RT3D Model Conclusions 40
7.0 Summary and Conclusions 41
8.0 References 42

Figures

Figure 1. Predicted Penetration Radius Based on Volume of Injected HRC 2
Figure 2. Relative Concentration versus Time at r_i = 5 ft (Linda, replace this figure) 6
Figure 3. Relative Concentration versus Time at r_i = 10 ft 7
Figure 4. Boundary Conditions and Injection Locations for Pilot Test Study 0514 10
Figure 5. Lactic Acid Concentration Plume at 25 days at Pilot Test Study Location 0514 11
Figure 6. Lactic Acid Concentration Plume at 88 days at Pilot Test Study Location 0514 11
Figure 7. Lactic Acid Concentration Plume at 25 days at Pilot Test Study Location 0526 12

Figure 8. Lactic Acid Concentration Plume at 88 days at Pilot Test Study Location 0526 12
Figure 9. Lactic Acid Concentration Plume at 25 days at Pilot Test Study Location S73C 13
Figure 10. Lactic Acid Concentration Plume at 88 days at Pilot Test Study Location S73C 13
Figure 11. Relative Concentration versus Time for each Pilot Test Well 14
Figure 12. Relative Lactic Acid Concentration versus Time at 0514 for Different Diffusion Coefficients 14
Figure 13. Barrier Wall Design with 10 ft Spacing 15
Figure 14. Barrier Wall Design with 12 ft Spacing 15
Figure 15. Barrier Wall Design with 15 ft Spacing 16
Figure 16. Relative Concentration Related to Barrier Wall Spacing with D=0.2 ft^2/day 17
Figure 17. Relative Concentration Related to Barrier Wall Spacing with D=0.002 ft^2/day 17
Figure 18. Base Map Showing Injection Points, Observation Points, and Boundary Conditions 19
Figure 19. MT3DMS—Vinyl Chloride (mg/L) at 120 days, Porosity=0.25 20
Figure 20. MT3DMS—Vinyl Chloride (mg/L) at 120 days, Porosity=0.05 20
Figure 21. Vinyl Chloride Concentration versus Time at Well 0514 21
Figure 22. MT3DMS—Organic Acid (mg/L) at 120 days, Porosity=0.25, Half-life=182.5 days 22
Figure 23. MT3DMS—Organic Acid (mg/L) at 120 days, Porosity=0.25, Half-life=365 days .. 22
Figure 24. Organic Acid Concentration versus Time at Well 0514 23
Figure 25. MT3DMS—Organic Acid (mg/L) at 120 days, Porosity=0.05, Half-life=182.5 days 23
Figure 26. MT3DMS—Organic Acid (mg/L) at 120 days, Porosity=0.05, Half-life=365 days .. 24
Figure 27. MT3DMS—Vinyl Chloride (mg/L) at 120 days, Porosity=0.25 25
Figure 28. MT3DMS—Vinyl Chloride (mg/L) at 120 days, Porosity=0.05 26
Figure 29. Vinyl Chloride Concentration versus Time at Well 0514 27
Figure 30. MT3DMS—Organic Acid (mg/L) at 120 days, Porosity=0.25, Half-life=182.5 days 28
Figure 31. MT3DMS—Organic Acid (mg/L) at 120 days, Porosity=0.25, Half-life=365 days .. 28
Figure 32. Organic Acid Concentration versus Time at Well 0514 29
Figure 33. MT3DMS—Organic Acid (mg/L) at 120 days, Porosity=0.05, Half-life=182.5 days 30
Figure 34. MT3DMS—Organic Acid (mg/L) at 120 days, Porosity=0.05, Half-life=365 days .. 30
Figure 35. Organic Acid Concentration versus Time at Well 0514 32
Figure 36. RT3D—Vinyl Chloride (mg/L) at 25 days F=10 34
Figure 37. RT3D—Vinyl Chloride (mg/L) at 88 days F=10 34
Figure 38. RT3D—Vinyl Chloride (mg/L) at 365 days F=10 35
Figure 39. RT3D—Organic Acid (mg/L) at 25 days F=10 35
Figure 40. RT3D—Organic Acid (mg/L) at 88 days F=10 36
Figure 41. RT3D—Organic Acid (mg/L) at 365 days F=10 36
Figure 42. RT3D—Vinyl Chloride (mg/L) at 25 days F=10000 37
Figure 43. RT3D—Vinyl Chloride (mg/L) at 88 days F=10000 37
Figure 44. RT3D—Vinyl Chloride (mg/L) at 365 days F=10000 38
Figure 45. RT3D—Organic Acid (mg/L) at 25 days F=10000 38
Figure 46. RT3D—Organic Acid (mg/L) at 88 days F=10000 39
Figure 47. RT3D—Organic Acid (mg/L) at 365 days F=10000 39
Figure 48. Organic Acid Concentration versus Time 40

Tables

Table 1. Relative Concentration at r_i = 5 ft 6
Table 2. Relative Concentration at r_i = 10 ft 7
Table 3. Estimated Diffusion Coefficient for Lactic Acid at Selected Temperatures 8
Table 4. Initial Component Concentrations 18
Table 5. Parameter Values for Concentration Plume Plots 21
Table 6. Porosity and Half-life Sensitivity at 120 Days 24
Table 7. Parameter Values for Concentration Plume Plots 26
Table 8. Porosity and Half-life Sensitivity at 120 Days 31
Table 9. Parameter Values for Diffusion Coefficient Curves 31
Table 10. Diffusion Coefficient Sensitivity at 120 Days 32
Table 11. MT3DMS Parameters 33
Table 12. Stoichiometric Ratio Sensitivity at 365 Days 40

Appendixes

Appendix A Justification for Low Porosity Analogy Between Preferred Flow Paths and Fractured Flow

1.0 Introduction

The modeling described in this document was conducted to simulate the enhanced bioremediation action for plume control currently underway in the southeast portion of the Building 100 Area at the Young - Rainey Science, Technology, and Research Center (STAR Center). The model will be used to predict the effects of enhanced bioremediation at this area. Additionally, the model may be used in the future to evaluate the applicability of enhanced bioremediation at other areas of the STAR Center. The model will aid the design and costing of the potential remediation systems, and will allow evaluation of the progress of the remediation once implemented.

Both the planned pilot testing of enhanced bioremediation in this area and the full-scale plume control remediation effort have been considered in the quantitative analyses. The remediation consists of injecting Hydrogen Release Compound (HRC) via temporary boreholes. HRC slowly releases lactic acid, which in turn breaks down to other acids. Lactic and other acids produce hydrogen that is used by microorganisms to biodegrade the contaminants. The simulations produced under the modeling effort serve not only to provide estimates of the ability of HRC and derivative acids to penetrate site porous media and influence organic contaminants, but also to develop refined estimates for hydraulic properties of the shallow surficial aquifer.

Simulation of the enhanced bioremediation efforts has focused on three general types of processes:

1. Advective movement of HRC away from injection sites for relatively short periods following injection,
2. The spatial distribution of lactic acid as it is released from injected HRC and subsequently affected by combined advective, dispersive, and diffusive transport processes, and
3. The eventual biologically-mediated reaction of lactic acid and other derivative acids with organic compounds, thereby decreasing concentrations of the latter.

The first of these process types is expected to occur primarily in radial directions away from the injection locations. The second type takes into account the spreading of lactic acid as it moves downgradient under ambient ground water flow conditions, and the third type accounts for associated effects on ambient levels of vinyl chloride in the areas reached by lactic or other acids.

2.0 Assessment of HRC Penetration

Before fate and transport models can be applied to simulate enhanced bioremediation, estimates of the area penetrated by HRC injection are developed using relatively simple quantitative methods. These methods comprise both simple estimates of the aquifer pore volume available to HRC and analytical solutions of radial flow. The latter take into account pressures at the injection site that result from either continuous injection rates or prescribed injection pressures. Once the radial areas estimated as being affected by the injection are identified, grid discretization in the fate and transport models can be assessed to determine the model grid spacing required to accurately simulate lactic acid migration.

2.1 Penetration Radius Based on Volume

Three different HRC loading rates, described as the mass of HRC injected into the surficial aquifer per linear foot of the injection well, were proposed for the pilot study. Assuming the density of HRC is 1.347 grams per cubic centimeter, or about 11.239 pounds per gallon (lbs/gal), these rates—4.5, 6.0, and 8.0 pounds per linear foot (lbs/linear ft)—were translated into volumetric loading rates of 0.400, 0.534, and 0.712 gallons per linear foot (gal/linear ft), respectively. These latter rates were in turn translated into radial penetration radii assuming that a cylindrical portion of the aquifer with a specified porosity is occupied by the HRC. Figure 1 shows the resulting radial distances of HRC penetration for various porosity values. For porosities typically ascribed to fine-grained sand aquifers, i.e., 0.20 to 0.40, the radial penetration distances range from about 0.2 to 0.4 feet (ft). These results suggested that the HRC would be located within a cylindrical volume with a diameter of 0.4 to 0.8 ft around each injection point.

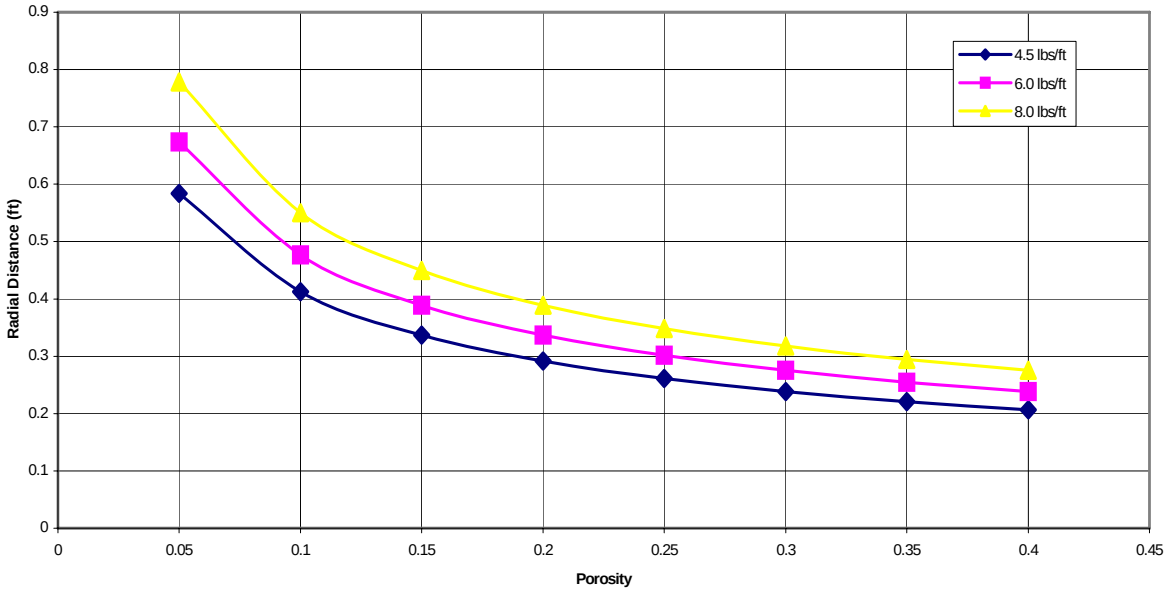

Figure 1. Predicted Penetration Radius Based on Volume of Injected HRC

2.2 Penetration Radius Based on Transport

Penetration radii for HRC were also estimated using a simple solution for radial advective transport of a dissolved constituent. This approach was not completely representative of actual conditions since HRC is injected as a separate-phase liquid that displaces water in the ground water system. However, it was believed to be appropriate for developing initial estimates of penetration.

The penetration radii developed using a transport solution were expected to be virtually the same as those estimated on the basis of HRC volume. However, unlike the volume approach, the transport methodology allowed the temporal aspects of HRC injection to be examined. It also allowed the permeability and depth characteristics of the surficial aquifer to be taken into

consideration. A prescribed injection rate boundary condition was applied with the transport solution. The injection rates were compared with ground water pumping rates that have historically been achieved from the surficial aquifer to assess whether they were feasible.

The modeling software WINFLOW (ESI 2000) was used to conduct the radial transport simulations. The rate at which HRC moved radially from an injection point was estimated by using a particle-tracking module to trace a molecule of liquid as it moved away from the injection point.

2.2.1 HRC Injection For Various Durations

Recovery well extraction rates at several of the sites within the STAR Center indicate that the aquifer will yield, on average, approximately 2 gallons per minute (gpm). Because HRC is more viscous than water, it is possible that the rate of injection of HRC will be less than this rate. To estimate the injection rates, the previously mentioned volumetric loading rates for HRC of 0.400, 0.534, and 0.712 gal/linear ft were initially adopted along with the assumption that it would take an average of one minute to inject the HRC in each vertical horizon at the injection well location. This approach produced injection rates of 0.400, 0.534, and 0.712 gpm, respectively.

These injection rates were applied using the Theis Equation solution in WINFLOW, which predicted hydraulic heads for various radii from the injection point at any prescribed time. The parameter values applied in the model were based on previous characterization studies at the site. These included: hydraulic conductivity (K) = 2.08 feet per day (ft/day), average aquifer saturated thickness (b) = 25 ft, aquifer storativity (S) = 0.003, and aquifer effective porosity (ne) = 0.20. At the end of 1 minute of injection, the penetration radii for the three volumetric injection rates were about 0.3, 0.35, and 0.4 ft, respectively, which are essentially identical to the penetration radii shown in Figure 1 for a porosity of 0.20 and the three proposed HRC loading rates. The pressure heads produced by the Theis solution in the uppermost 1 ft of saturated thickness about 0.4 ft from the injection point were about 1.5 to 2.5 ft, indicating that the injection of HRC would not cause problematic mounding of ground water.

The effect of varying injection times was also examined using the Theis model in the WINFLOW package. This was achieved by assuming that 8 pounds of HRC per linear ft of aquifer depth would be injected into the surficial aquifer for injection durations of 0.5, 1 and 2 minutes. These durations and the HRC loading rate translated into volumetric injection rates of 1.42, 0.72, and 0.36 gpm, respectively. The aquifer parameters used with this latter set of simulations were identical to those used earlier for the case in which all injection loading rates were applied over a duration of 1 minute. As with the earlier simulations, the variable injection durations produced no simulations in which ground water mounding would be a problem. The first of these simulations also indicated that an HRC mass loading rate of 8 lbs/linear ft for a duration of 0.5 minutes was feasible. As expected, the penetration radii predicted by these model runs fell in the range of 0.2 to 0.4 ft.

2.2.2 Radial Transport Summary

The WINFLOW results using prescribed HRC loading rates indicate that the proposed injection rates are feasible for the aquifer characteristics at the STAR Center. Simulation results also suggested that a cylindrical volume of HRC with a diameter of 0.4 to 0.8 ft could be expected

around each injection point. It follows logically that the actual diameter of each cylinder would be smaller than predicted if the actual HRC loading rates were lower than proposed, or larger if the actual injection rates were larger than proposed rates. It also stands to reason that the radius of HRC penetration will vary with depth if some HRC mass loading rates or effective porosities are greater in some horizons than in others.

3.0 Lactic Acid Migration

The assessment of HRC injection was followed with analyses of transport in ground water of the organic acids generated from the HRC. These analyses centered on estimating the spatial distribution of the acid over time as affected by various natural processes occurring in the surficial aquifer. Relatively widespread distribution of the acids is necessary if enhanced biodegradation of chlorinated ethenes in the target areas is to be completely successful.

3.1 Diffusion of Lactic Acid

According to Regenesis literature (Regenesis TB 2.8.2), much of the success of HRC injection in reducing concentrations of chlorinated solvent contaminants is related to the ability of the acids generated by the HRC to spread over large areas relatively rapidly. Spreading makes it possible for the acids to come in contact with the dissolved contaminants and for hydrogen atoms in the acids to act as electron donors in the bacterial degradation processes that ensue. During degradation, hydrogen atoms replace chlorine atoms in the chemical structure of contaminants such as perchlorethene (PCE), trichlorethene (TCE), dichlorethene (DCE), and vinyl chloride, in a process referred to as reductive dechlorination (Regenesis TB 1.1.2).

3.1.1 Relative Concentration

In the analysis below, the relative acid concentration at a specified distance is used to show how the acids migrate. The analysis is based on the analogy or relationship between:

1) The drawdown ($h_{rw} - h_0$) at a free-flowing well and drawdown ($h_{ri} - h_0$) at a distance r_i
2) The initial concentration (C_0) at the well and concentration (C) at a distance r_i

The equation for discharge Q of a free-flowing well (Kruseman 1991) is:

$$Q = 2 \times \pi \times T \times (h_r - h_0) \times G(u)$$

The function G(u) can be approximated by 2 / W(u) for all but extremely small values of time t. W(u) is know as the well function (Freeze 1979). Transmissivity T has dimension of [length^2/time].

Therefore:

$$Q = 4 \times \pi \times T \times (h_r - h_0) / W(u)$$

This can be expressed at the well with a radius r_w as:

$$Q = 4 \times \pi \times T \times (h_{rw} - h_0) / W(u_{rw}) \qquad \text{Equation (1)}$$

At any radii r_i this can be expressed as:

$$Q = 4 \times \pi \times T \times (h_{ri} - h_0) / W(u_{ri}) \qquad \text{Equation (2)}$$

Setting Equation (1) = Equation (2)

$$4 \times \pi \times T \times (h_{rw} - h_0) / W(u_{rw}) = 4 \times \pi \times T \times (h_{ri} - h_0) / W(u_r i)$$

or

$$h_{rw} - h_0 / W(u_{rw}) = h_{ri} - h_0 / W(u_r i)$$

Substituting C_0 for ($h_{rw} - h_0$) and C for (hri – h_0)
where C_0 is the concentration at the well
and C is the concentration at a distance r_i
yields

$$C_0 / W(u_{rw}) = C / W(u_{ri})$$

or

$$C / C_0 = W(u_{ri}) - W(u_{rw})$$

By definition:

$$u = (r^2 \times S) / (4 \times T \times t)$$

where storativity S is dimensionless. Hydraulic diffusivity D, also known as the diffusion coefficient, is defined as T/S and has dimensions of [length^2/time].

Substituting 1 / D for S / T

yields

$$u = r^2 / (4 \times D \times t)$$

or

$$u_{rw} = r_w{}^2 / (4 \times D \times t) \quad \text{and} \quad u_{ri} = r_i{}^2 / (4 \times D \times t)$$

For the analysis here: r_w = 0.4 ft
r_i = 5.0 and 10.0 ft
D = 2.0, 0.2, and 0.02 ft^2/day
t = 30, 60, 90, 120, 150, 180, 210, 240, 270, 300, 330, and 360 days
The values selected for D are one order of magnitude above and below the value claimed by Regenesis.

In Table 1 and Figure 2 below, r_i = 5.0 ft.

Table 1. Relative Concentration at r_i = 5 ft

Time (days)	Relative Concentration (C/C_0) with		
	D = 2.0 ft^2/day	D = 0.2 ft^2/day	D = 0.02 ft^2/day
30	0.265125	0.046097	0.000001
60	0.326955	0.104343	0.000315
90	0.359622	0.144525	0.002219
120	0.381253	0.173954	0.006150
150	0.397182	0.196778	0.011615
180	0.409667	0.215229	0.018020
210	0.419866	0.230605	0.024915
240	0.428445	0.243716	0.032005
270	0.435820	0.255100	0.039103
300	0.442270	0.265125	0.046097
330	0.447986	0.274060	0.052919
360	0.453110	0.282101	0.059532

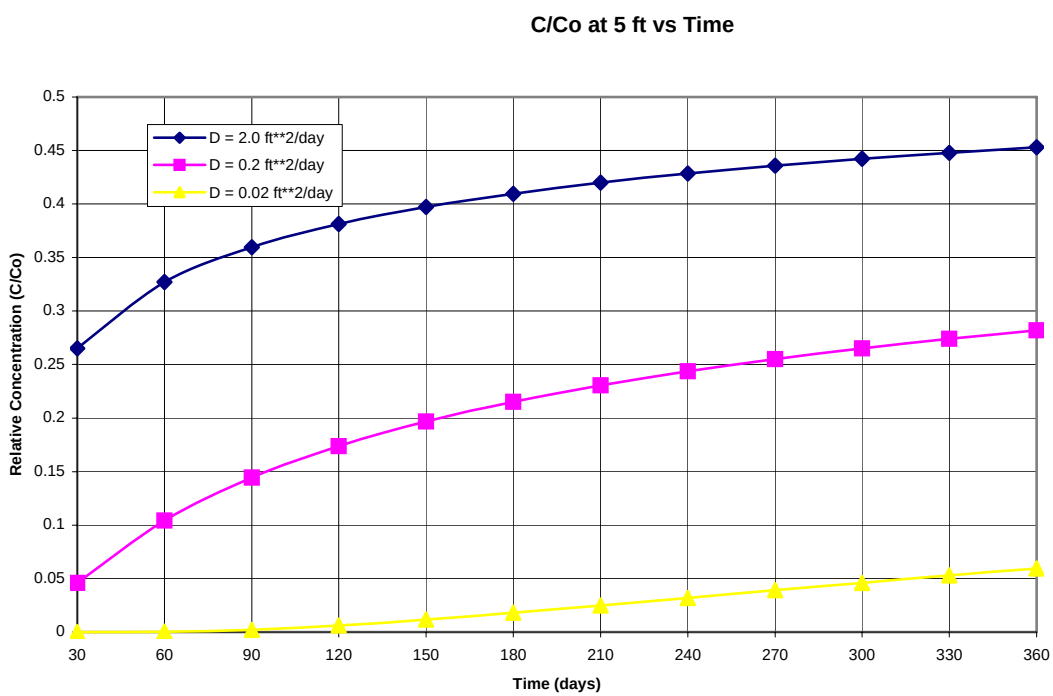

Figure 2. Relative Concentration versus Time at r_i = 5 ft

In Table 2 and Figure 3 below, r_i = 10.0 ft.

Table 2. Relative Concentration at r_i = 10 ft

Time (days)	Relative Concentration (C/C_0) with		
	D = 2.0 ft^2/day	D = 0.2 ft^2/day	D = 0.02 ft^2/day
30	0.100234	0.000696	0.000000
60	0.160087	0.008499	0.000000
90	0.195419	0.021357	0.000000
120	0.219892	0.035159	0.000001
150	0.238368	0.048403	0.000007
180	0.253084	0.060668	0.000031
210	0.265240	0.071903	0.000093
240	0.275549	0.082176	0.000213
270	0.284469	0.091586	0.000410
300	0.292308	0.100234	0.000696
330	0.299287	0.108212	0.001079
360	0.305563	0.115602	0.001561

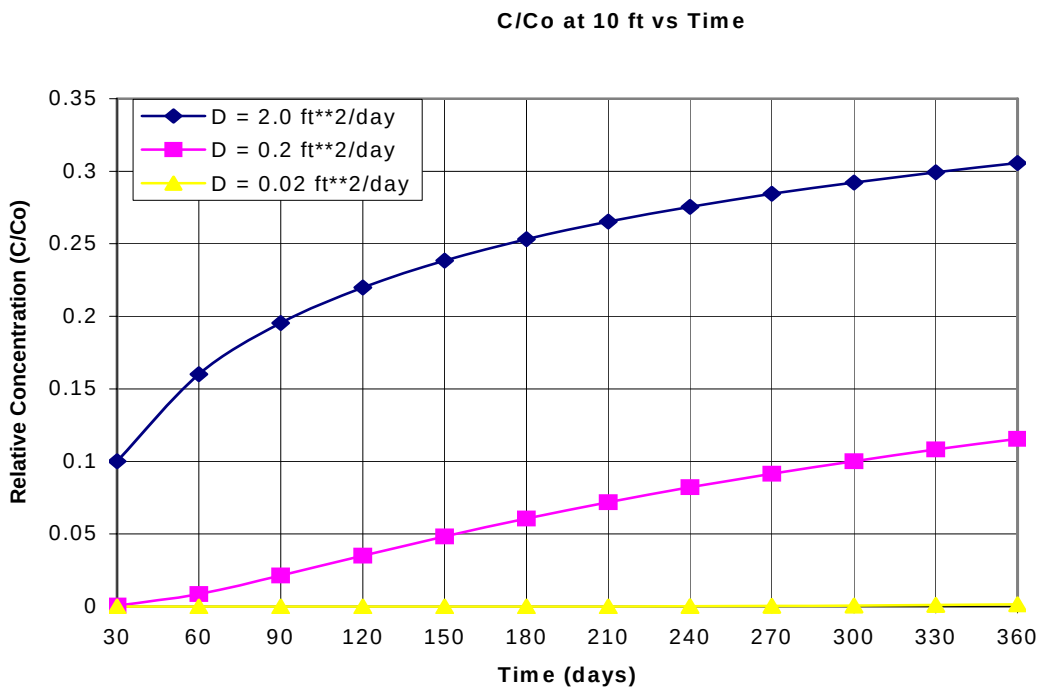

Figure 3. Relative Concentration versus Time at r_i = 10 ft

3.1.2 Estimated Lactic Acid Diffusion Coefficient

The diffusion coefficient of lactic acid was estimated as a further check on the reasonability of the 0.2 ft^2/day claimed by Regenesis. The diffusion coefficient of organic compounds in water can be estimated by the method of Hayduk and Laudie (1974). For lactic acid, Table 3 shows the estimated values for different temperatures.

Table 3. Estimated Diffusion Coefficient for Lactic Acid at Selected Temperatures

Temperature		Estimated Diffusion Coefficient	
Deg. C	Deg. F	cm^2/sec	ft^2/day
0	32	0.46711×10^{-5}	0.43442×10^{-3}
5	41	0.56217×10^{-5}	0.52282×10^{-3}
10	50	0.66725×10^{-5}	0.62055×10^{-3}
15	59	0.78056×10^{-5}	0.72593×10^{-3}
20	68	0.90355×10^{-5}	0.84012×10^{-3}
25	77	0.10335×10^{-4}	0.96118×10^{-3}
30	86	$0.11719 \times 1\ 0^{-4}$	0.10898×10^{-2}

The published range in Freeze and Cherry (1979) for major ions in ground water is 1×10^{-5} to 2×10^{-5} cm^2/sec or 9.3×10^{-4} to 1.86×10^{-3} ft^2/day at 25 degrees C.

3.2 Conclusions

Figures 2 and 3 and Tables 1 and 2 show that the diffusion coefficient has a significant affect on the relative concentration at five and 10 ft from the injection location for times up to 1 year. It is clear from these data that the relative concentration for a diffusion coefficient < 0.02 ft^2/day is virtually zero at any distance greater than 10 ft. It follows logically that the spreading of lactic acid is not primarily due to diffusion, but must be dominated by advection-dispersion processes. Advective-dispersive modeling is presented in Section 5.0.

The estimated diffusion coefficient for lactic acid shown in Table 3 for different temperatures does not support the value of 0.2 ft^2/day reported by Regenesis. This is another indication that spreading is not solely the result of diffusion.

4.0 Pilot Test Study Modeling

The original design of the pilot test consisted of nine injection points located around each of three existing monitoring wells. The planned injection point spacing design was different at each well, with one set of injection points spaced 10 ft apart on center, one set spaced 12 ft apart, and one set spaced 15 ft apart. The purpose of this was to test the effectiveness of each design so that the most appropriate design (balancing cost and effectiveness) could be applied to the full-scale plume control design.

Once in the field, however, slight modifications to the location of individual injection points were necessary due to the presence of buried utility lines and various landscaping features. The westernmost row of injection points at well 0514 (10 ft spacing) was shifted approximately 2 ft to the east and 1 ft to the south because of utility lines and bushes. At well S73C, the original design was changed due to regulatory requirements: the easternmost row of injection points was moved 45 ft to the west to become the westernmost row of points. Subsequently, this westernmost row of injection points (15 ft spacing) was shifted approximately 3 ft to the east due to a gas line. Also at this location, the southernmost two injection points in the easternmost row were shifted approximately 1 ft to the west to avoid damage to landscaping. Injection points

around well 0526 (12 ft spacing) were not moved. These slight modifications to injection point spacing are reflected in the models.

4.1 Combined Advective-Dispersive Transport of Lactic Acid

Three flow and transport models have been used to model HRC injection as installed in the field at pilot test locations 0514, 0526, and S73C, respectively. The injection point locations for the models approximate the actual injection point spacing as close as possible with a 0.5 ft model grid spacing. The analysis that follows shows how the predicted relative concentration (C/Co) of HRC (or the acids that form from HRC) varies at the associated pilot test well.

It should be noted that most of the modeling conducted under this part of the investigation provided optimistic predictions of the spatial distribution of HRC-generated acids over time. This is because most simulations were designed to approximate the effects of preferred flow paths in ground water media at the site. This was accomplished by assuming the porosity of the surficial aquifer was only 0.05 (5 percent), when, in fact the actual porosity is closer to a value of 0.3 to 0.4 (30 to 40 percent). Because pore-water velocity in the aquifer is inversely proportional to porosity, the adoption of a 5 percent porosity meant that predicted transport velocities and, therefore, transport distances, could be 6 to 8 times larger than would be predicted using actual porosity values. Though this approach to the modeling made it possible to explain the possible presence of organic acids at relatively large distances from HRC injection points, it did have drawbacks that are important to mention.

Inherent in the assumption that preferred flow paths exist at the site is that chemicals will migrate in alluvial ground water in the same manner that they would be transported through fractured rock (see Appendix A). That is, the chemicals would be expected to move quickly through the preferred flow paths, which are analogous to rock fractures, but would diffuse very slowly into less permeable zones between the preferred paths, which are analogous to the rock matrix between fractures. Consequently, the predicted areal extents of HRC-generated acids presented in this section of the study account only for acid present in the preferred flow paths, but do represent acid between paths. Accordingly, it is possible that the computed acid concentrations assumed to have an effect on chlorinated ethenes in less permeable zones would actually have no effect at all. This potential disconnection between model predictions and actual conditions should be kept in mind while reviewing the findings presented in this report sections, and in subsequent sections dealing with the ability of hydrogen in the acids to replace chlorine atoms in the site's contaminants.

The flow and transport parameters and conditions are:

- $K_x = K_y = 2.08$ ft/day
- Porosity = 0.05 (see Appendix A for explanation for low porosity value)
- Hydraulic Gradient = 0.004
- No-flow boundaries on northeast and southwest side of model (see Figure 4)
- Constant Head = 7.0 ft at northwest boundary of model (see Figure 4)
- Constant Head = 6.6 ft at southeast boundary of model (see Figure 4)
- No Recharge
- No Evapotranspiration
- Longitudinal Dispersivity = 5.0 ft, Transverse Dispersivity = 0.5 ft

- $K_d = 0.0$
- Bulk Density (of the porous medium in the aquifer) = 0.0
- No initial concentration for HRC (or the acids that form from HRC)
- Top elevation gradient of 0.004 from northwest (17.0 ft) to southeast (16.6 ft) of model
- Bottom elevation gradient of 0.004 from northwest (-43.0 ft) to southeast (-43.4 ft) of model
- **Diffusion Coefficient = 0.2 ft^2/day (Regenesis literature value)**
- **9 Constant Concentration Cells = 1.0 (to represent the HRC injection points)**
- **There is no HRC (or acid) degradation**

The last three items (**bold type**) in the list above are the most critical assumptions.

A base map showing the boundary conditions and the injection locations for pilot test study area 0514 is displayed in Figure 4 below. The flow direction is from northwest to southeast.

A single observation location corresponding to the monitoring well location was used in each model to capture the predicted lactic acid concentration at specified times. Some of the specified times correspond to the planned or projected sampling events. Other times were selected to fill the intervals between sampling events. Figures 5 and 6 show the lactic acid concentration plume at well 0514 at two planned sampling event times of 25 and 88 days, respectively. Figures 7 and 8 show the concentration plume at well 0526 at 25 and 88 days, respectively. Figures 9 and 10 show the concentration plume at well S73C at 25 and 88 days, respectively.

In general, the injection spacing is closest at pilot test location 0514, then at 0526, and farthest at S73C. As expected, the closer the injection spacing the higher the concentration between the injection locations.

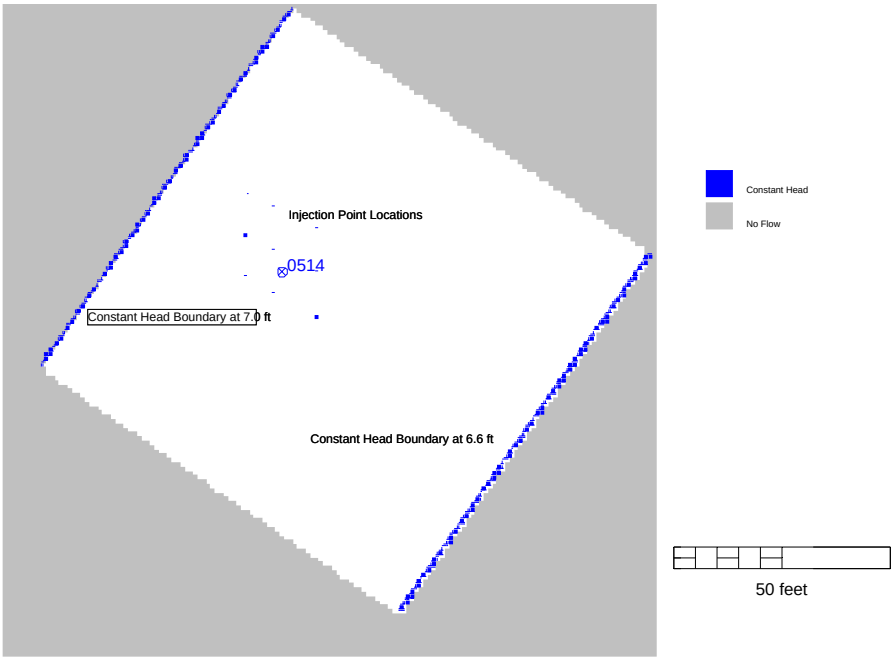

Figure 4. Boundary Conditions and Injection Locations for Pilot Test Study 0514

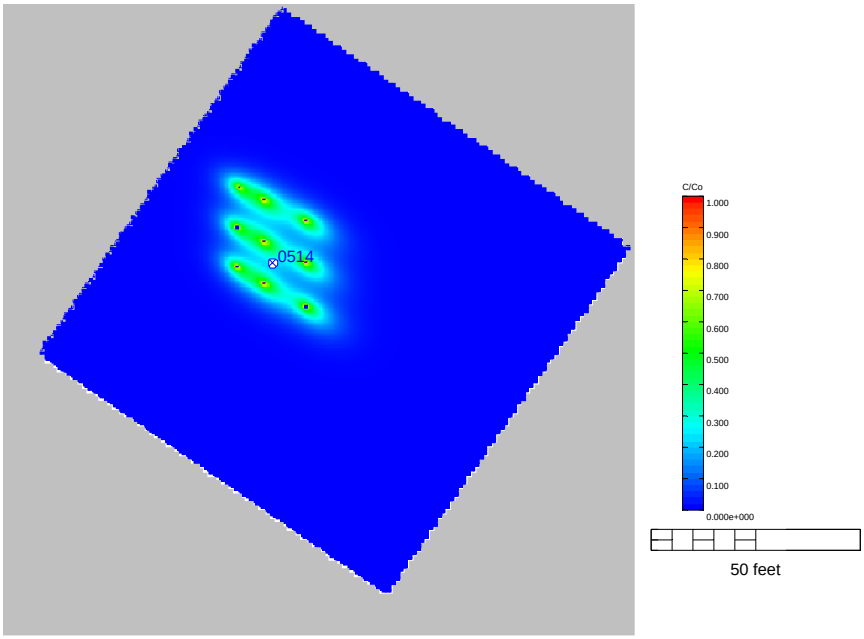

Figure 5. Lactic Acid Concentration Plume at 25 days at Pilot Test Study Location 0514

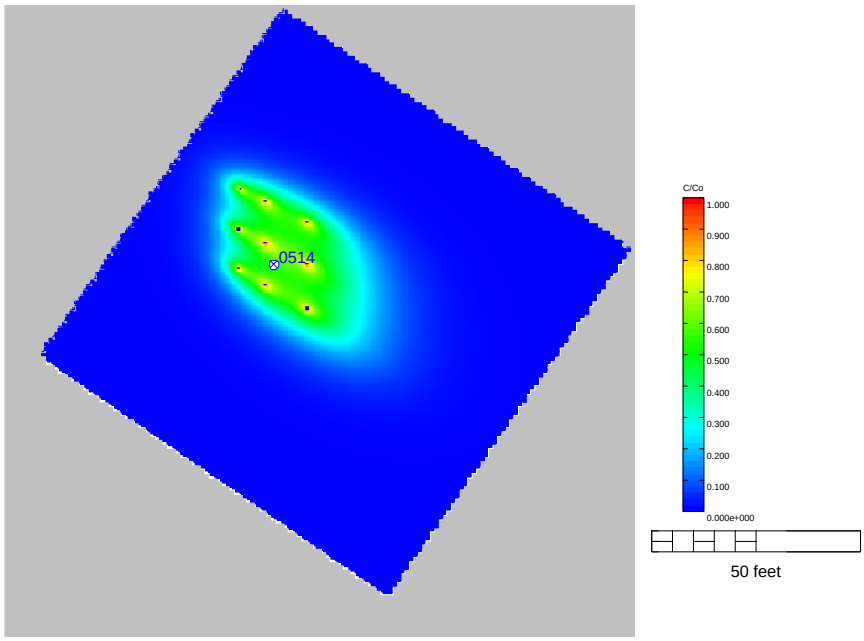

Figure 6. Lactic Acid Concentration Plume at 88 days at Pilot Test Study Location 0514

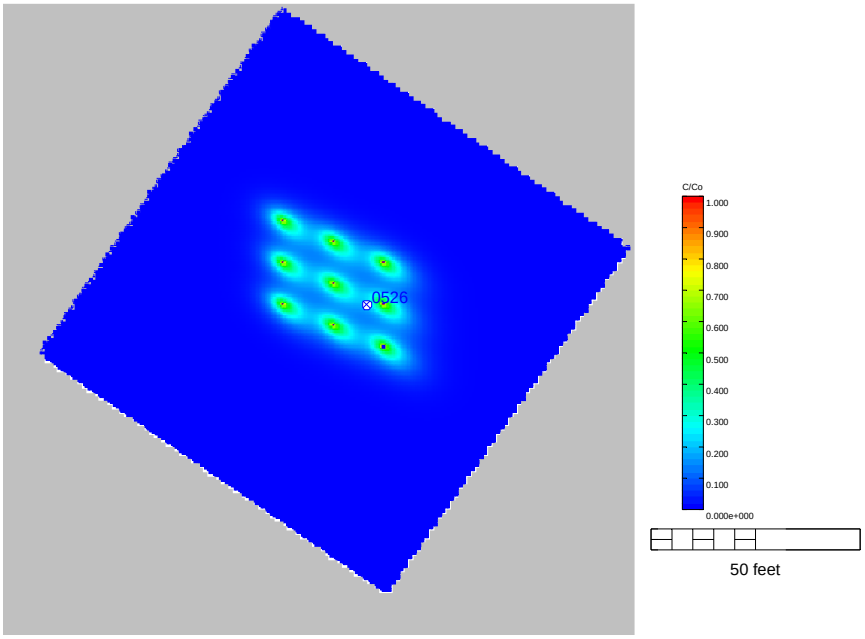

Figure 7. Lactic Acid Concentration Plume at 25 days at Pilot Test Study Location 0526

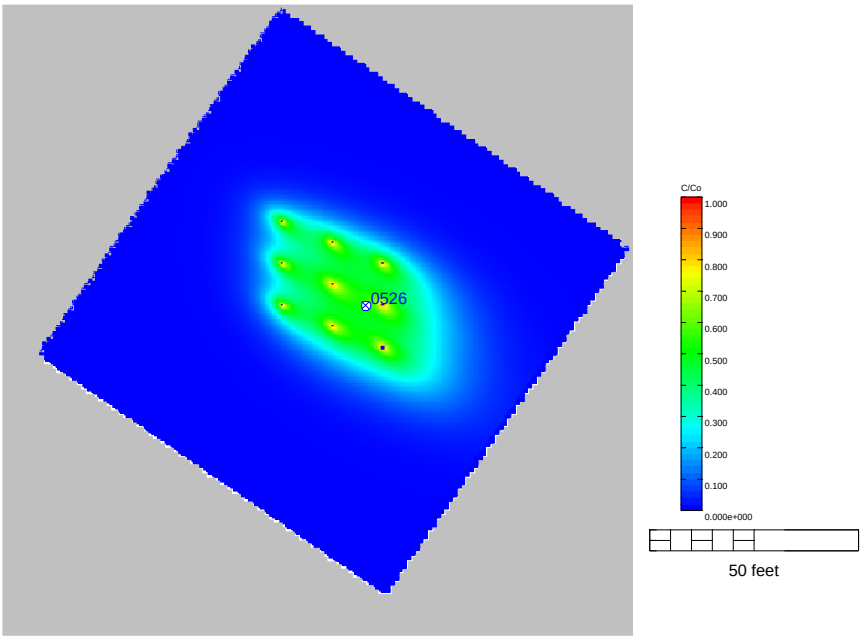

Figure 8. Lactic Acid Concentration Plume at 88 days at Pilot Test Study Location 0526

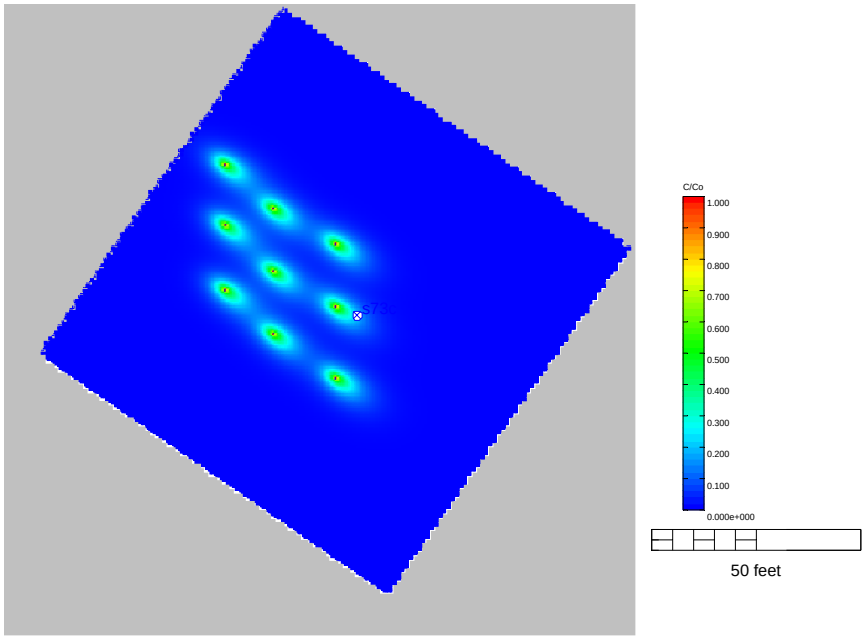

Figure 9. Lactic Acid Concentration Plume at 25 days at Pilot Test Study Location S73C

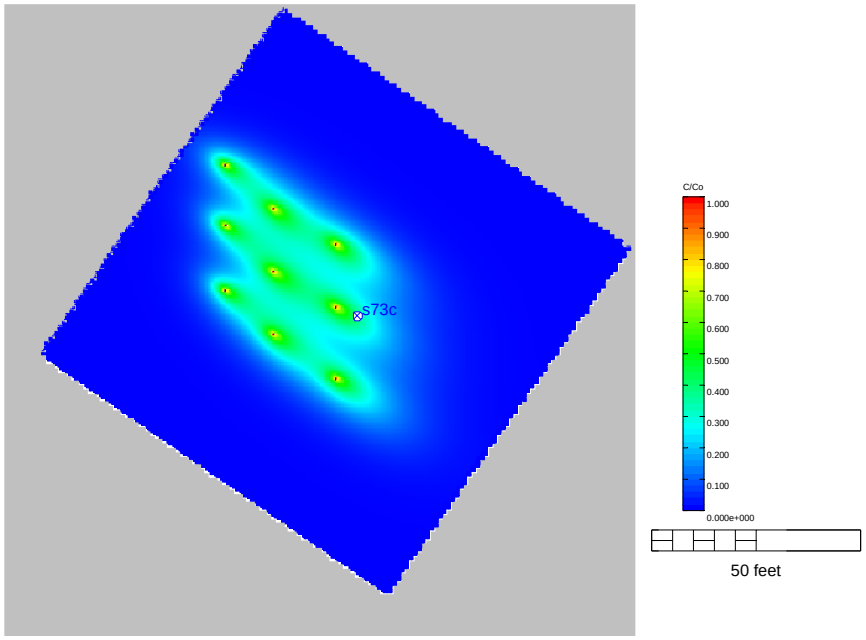

Figure 10. Lactic Acid Concentration Plume at 88 days at Pilot Test Study Location S73C

Figure 11 displays the relative concentration versus time for the observation location in each pilot test area. The 3/14/03 date is the approximate and assumed date that the HRC injection was completed at the pilot test areas. Observed field data, when received, can be plotted on this chart

to compare with simulated data. This information will be used to adjust transport parameters such as porosity, dispersivity, diffusion coefficient, etc., to calibrate the transport models.

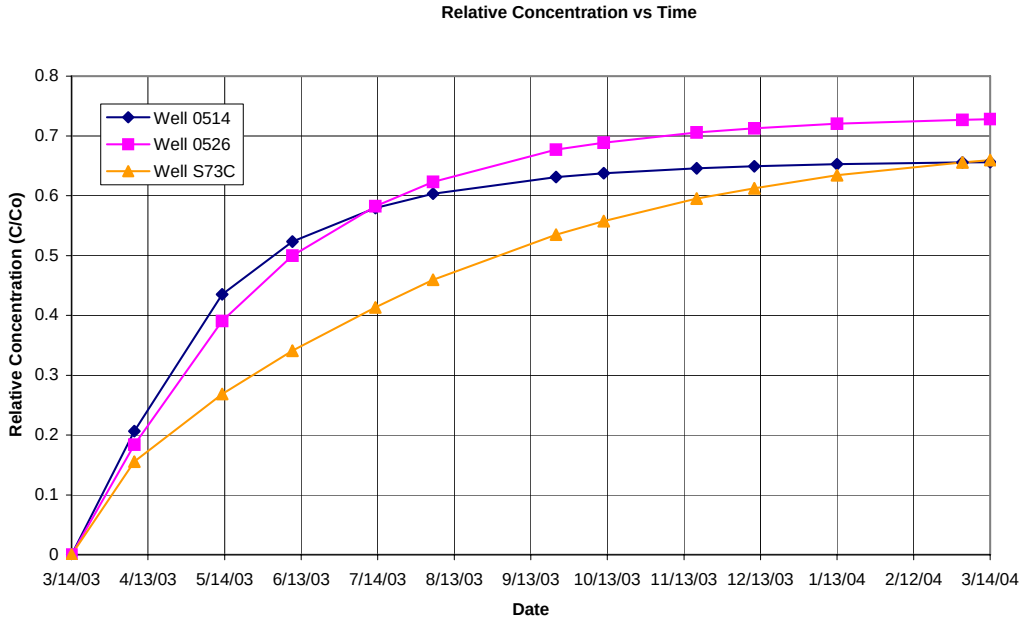

Figure 11. Relative Concentration versus Time for each Pilot Test Well

4.2 Diffusion Coefficient Sensitivity Analysis

To demonstrate the difference that the diffusion coefficient can have on the relative concentration, results for three values of diffusion coefficient are shown in Figure 12 for pilot test area 0514. This figure demonstrates the significant difference in the relative concentration for one and two orders of magnitude reduction from the Regenesis diffusion coefficient value of 0.2 ft^2/day, particularly in days immediately after injection. The smallest diffusion coefficient value of 0.002 ft^2/day is close to the upper limit reported in the literature.

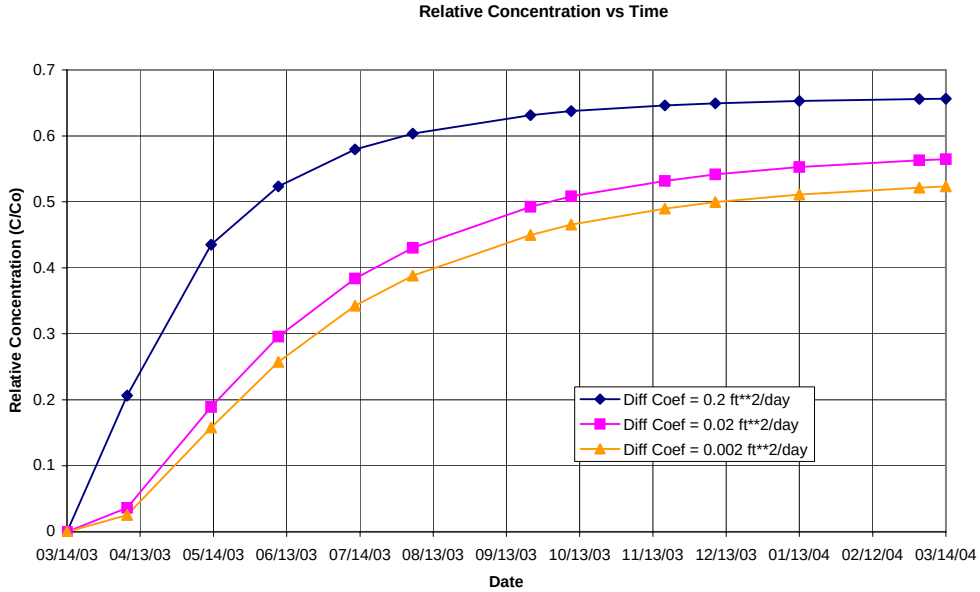

Figure 12. Relative Lactic Acid Concentration versus Time at 0514 for Different Diffusion Coefficients

4.3 Full Scale Barrier Wall Design

The proposed barrier wall in the full scale plume control task will be created by injecting HRC along two offset rows of injection points. The spacing between points (either 10 ft, 12 ft, or 15 ft) will be selected based on the results of the pilot test. Three simple models have been constructed following this design concept with 10 ft, 12 ft, and 15 ft spacing. These models are shown in Figures 13, 14, and 15, respectively.

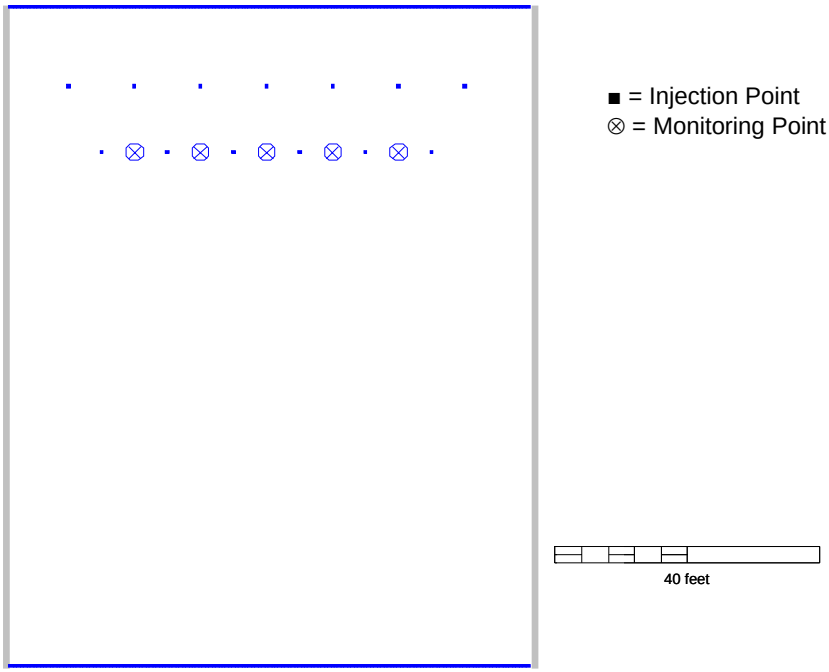

Figure 13. Barrier Wall Design with 10 ft Spacing

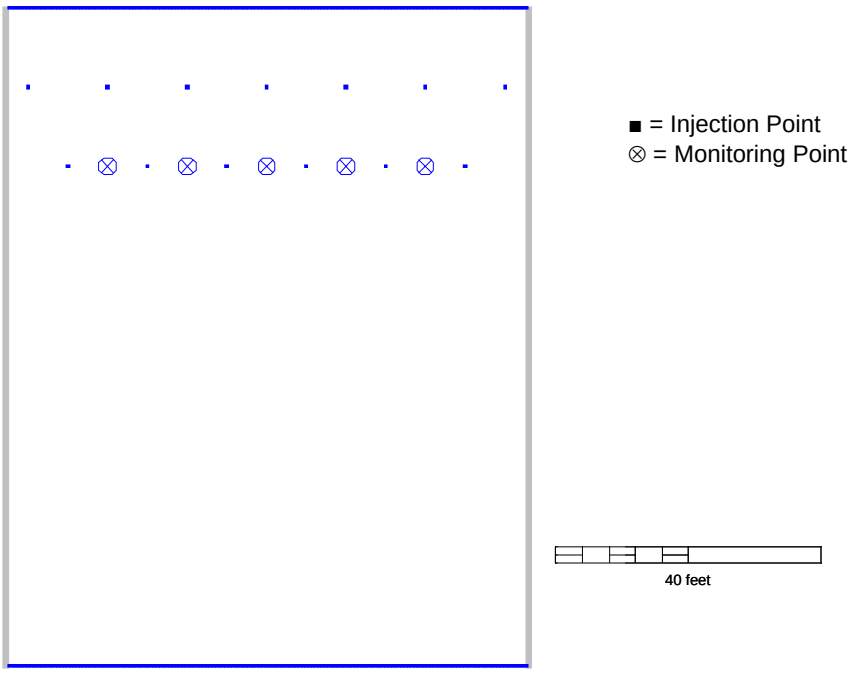

Figure 14. Barrier Wall Design with 12 ft Spacing

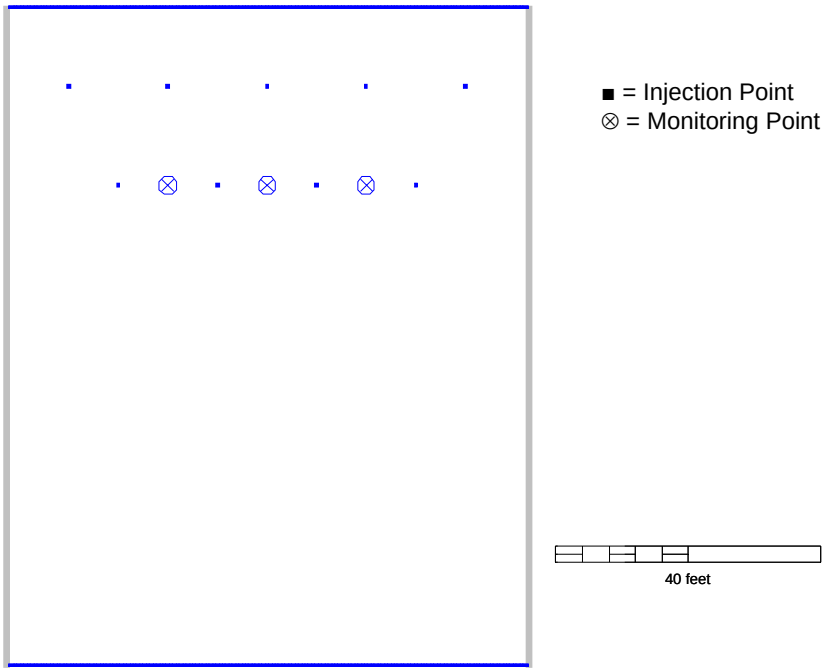

Figure 15. Barrier Wall Design with 15 ft Spacing

Each model was run to calculate the predicted relative concentration at the observation points that are midway between the injection points in the bottom row. The results, shown in Figures 16 and 17, indicate that the relative lactic acid concentration at any specific time is significantly higher for smaller injection spacing. Results are shown for two values of diffusion coefficient, 0.2 ft^2/day, the Regenesis claimed value, and 0.002 ft^2/day, a diffusion coefficient consistent with the upper range of published literature values.

4.4 Conclusions

The results of the pilot test modeling shown in Figure 11 need some explanation. Recall that the injection point spacing is closest at 0514 and furthest at S73C. Logically it would be expected that the relative concentration at any time would be higher for closer injection well spacing. And this would be true if the observation points were midway between the injection locations. However, for the pilot test models the observation points are not midway between injection locations. This explains why the relative concentration at 0526 is greater than at 0514 for times greater than four months.

The results of the barrier wall design modeling are as expected. Several obvious conclusions can be drawn from these results. The results with a diffusion coefficient of 0.002 ft^2/day are lower than with a diffusion coefficient of 0.2 ft^2/day. This is expected, but the magnitude is significant. For example, at 120 days the relative concentration is approximately 32 percent lower. In addition, the relative concentration is lower with wider row and injection point spacing. At 120 days, the relative concentration at 12 ft and 15 ft spacing is approximately 19 percent and 40 percent lower, respectively than the 10 ft spacing relative concentration.

Additionally, the barrier wall modeling demonstrates that the lactic acid will be dispersed throughout the entire area between injection points, indicating that an effective treatment zone will be established to control the plume.

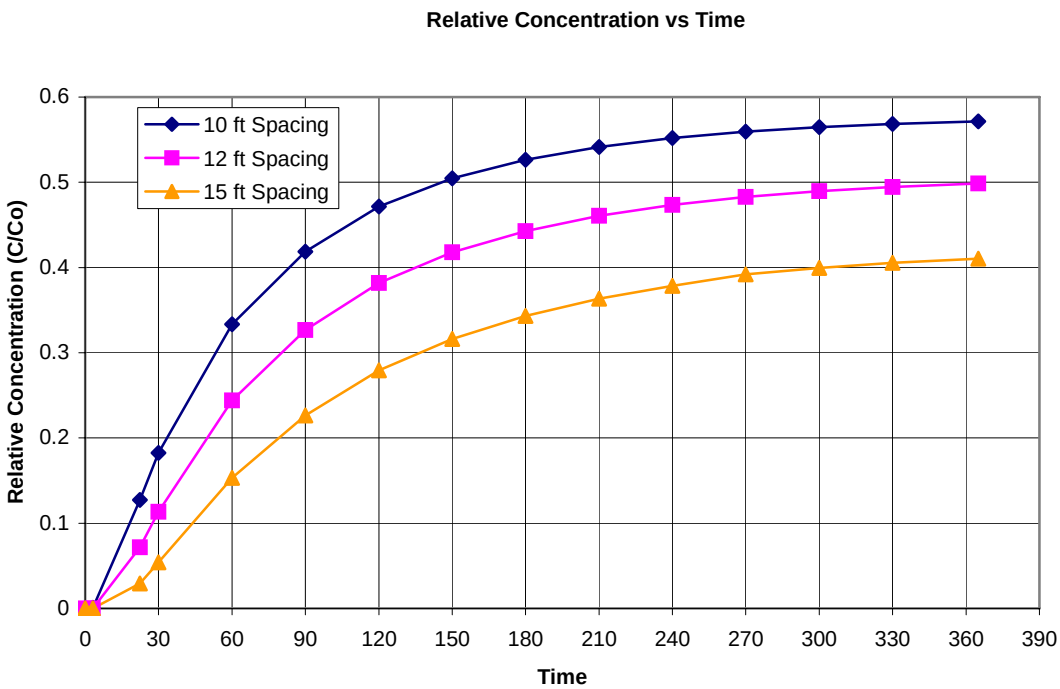

Figure 16. Relative Concentration Related to Barrier Wall Spacing with D=0.2 ft^2/day

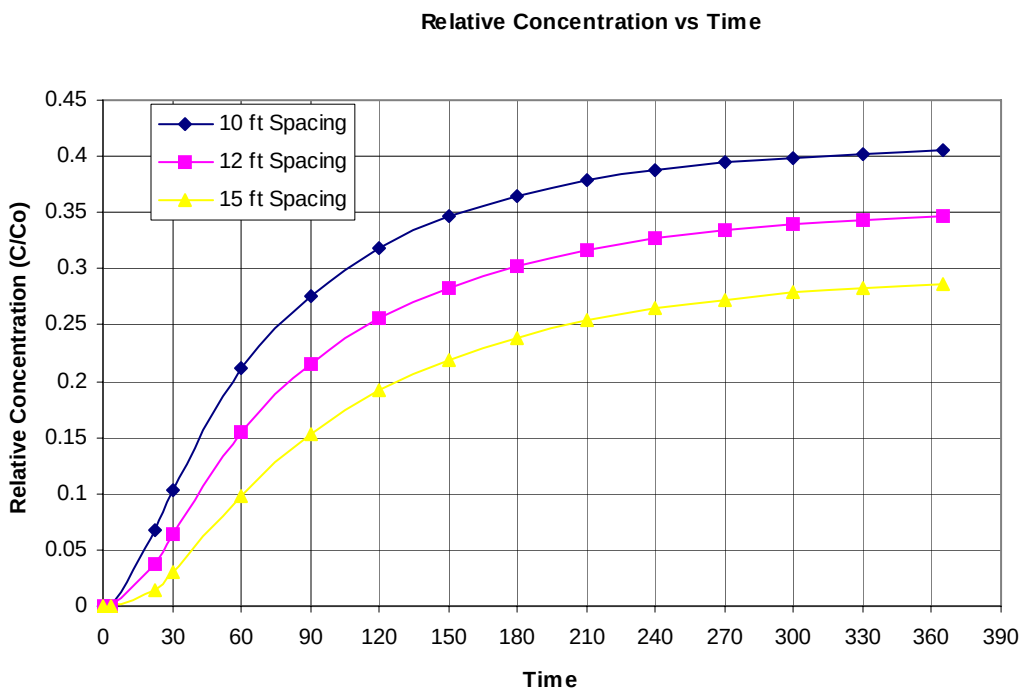

Figure 17. Relative Concentration Related to Barrier Wall Spacing with D=0.002 ft^2/day

5.0 MT3DMS Basic Advective-Dispersive Modeling

This multi-species two-component modeling was untaken for several purposes.

The primary purpose is to generate an initial concentration plume for two components that could be used as input to an RT3D instantaneous reaction model. Components 1 and 2 represent vinyl chloride and HRC/Lactic Acid/Hydrogen, respectively. Throughout this report, component 2 will be referred to as a hypothetical organic acid although the breakdown of HRC produces lactic acid $\rightarrow$ pyruvic acid $\rightarrow$ acetic acid, with hydrogen (H_2) released at each step.

The analysis will also show how sensitive the predicted concentration of vinyl chloride and the organic acid are to changes in parameter values. The parameters of interest are the diffusion coefficient, porosity, and the decay rate (λ) expressed as half-life. Two values were used for each parameter.

The initial component concentrations for this MT3DMS model are shown in Table 4.

Table 4. Initial Component Concentrations

Type of Property or Boundary Condition	Vinyl Chloride Concentration (mg/L)	Organic Acid Concentration (mg/L)
Initial Concentration	0.1	0.0
Constant Head at 9 Injection Locations	0.1	1000.0
Constant Head along Northwest	0.1	0.0
Constant Head along Southeast	0.1	0.0

A lag time of 120 days was used in the model to simulate the effects of non-contaminant electron demands, such as nitrate, sulfate, iron, etc. These demands must be at least partially satisfied before the hydrogen released from the organic acid can be used by the microorganisms to degrade vinyl chloride.

There is no decay rate associated with vinyl chloride. The decay rate associated with the organic acid is to account for the use of hydrogen by electron reductive reactions that must occur before or simultaneously with reductive dechlorination. The species that cause these reactions include but are not limited to nitrate, manganese, iron, and sulfate, in addition to the reductive dechlorination of PCE, TCE, DCE, and vinyl chloride. It is recognized that these reactions are not mutually exclusive and that several can occur simultaneously.

A base map showing the HRC injection points, observation points, and boundary conditions is shown in Figure 18.

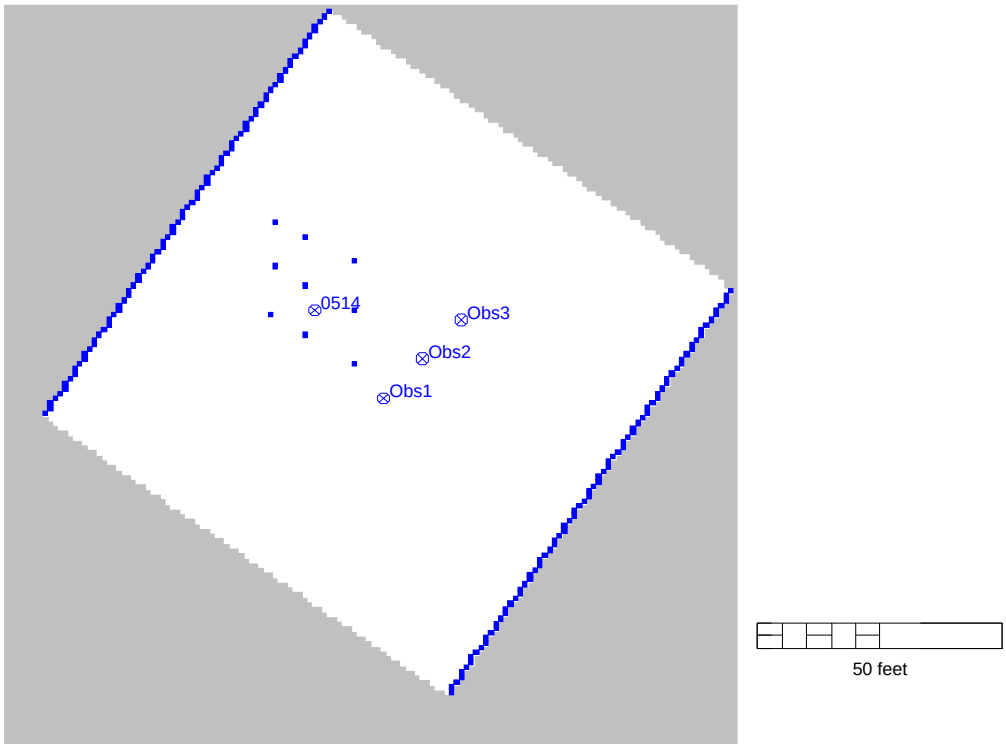

Figure 18. Base Map Showing Injection Points, Observation Points, and Boundary Conditions

5.1 Diffusion Coefficient = 0.2 ft^2/day

The vendor of HRC claims a lactic acid diffusion coefficient of 0.2 ft^2/day, which is at least two orders of magnitude greater than published literature values. This diffusion coefficient value will be used in this part of the analysis.

5.1.1 Component 1—Vinyl Chloride

Figures 19 and 20 show the concentration plume of vinyl chloride at 120 days with different parameter values as shown in Table 5. Despite the parameter differences these figures appear to be identical. The concentration versus time plot in Figure 21 shows a slight difference at location 0514 (note the scale). In general, all the concentration plots of vinyl chloride at 120 days looked to be identical regardless of how porosity and the half-life values vary. This is to be expected because there is no reaction between the two components (vinyl chloride and the organic acid) and there is not a decay rate associated with vinyl chloride.

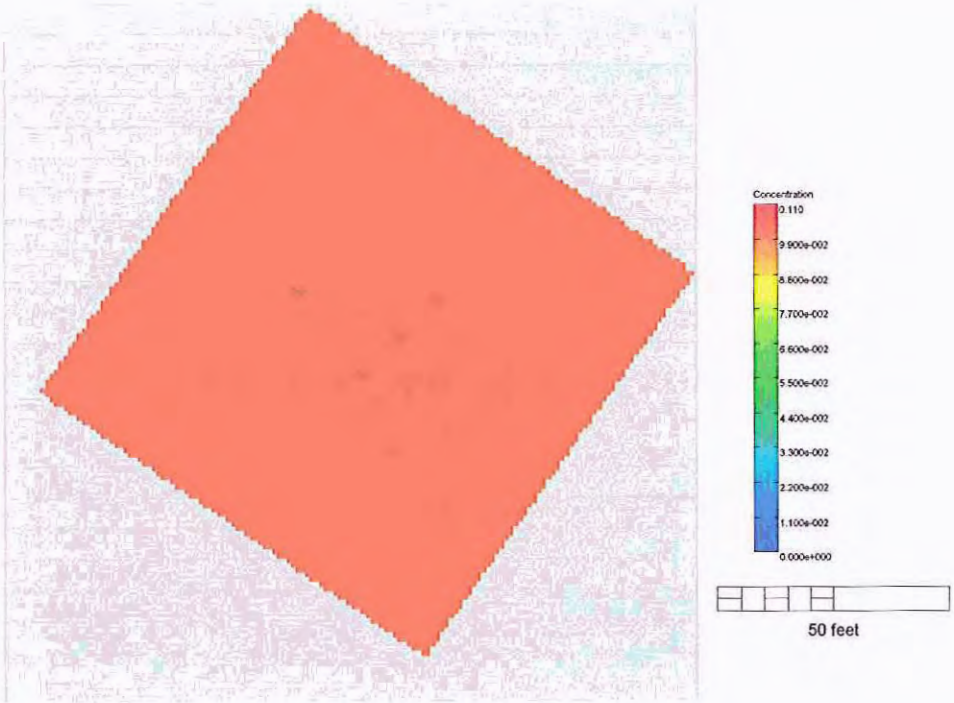

Figure 19. MT3DMS—Vinyl Chloride (mg/L) at 120 days, Porosity=0.25

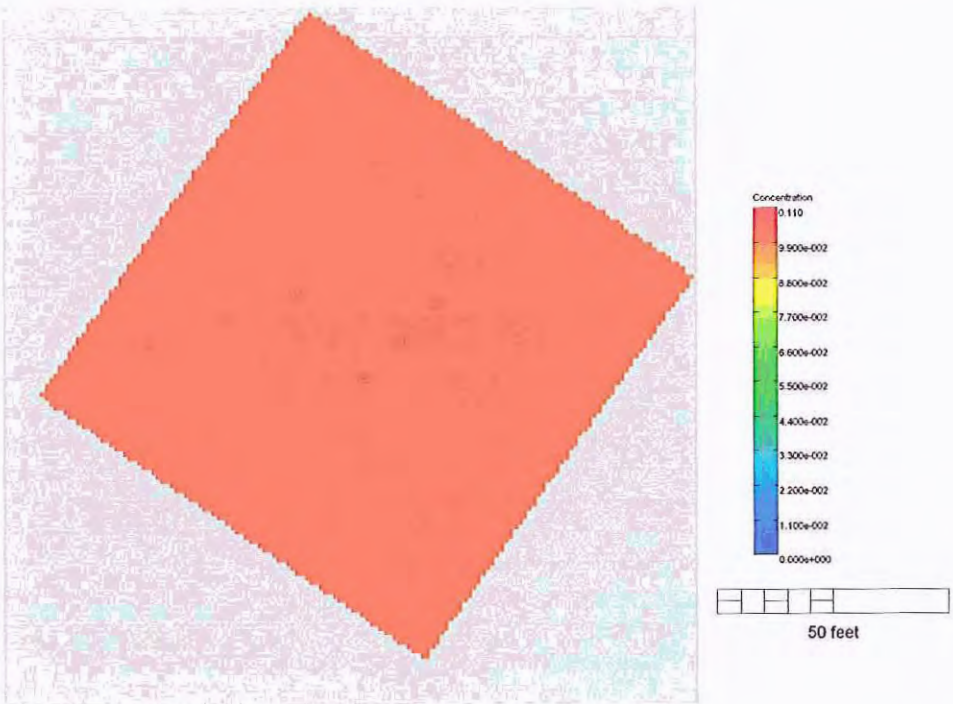

Figure 20. MT3DMS—Vinyl Chloride (mg/L) at 120 days, Porosity=0.05

Table 5. Parameter Values for Concentration Plume Plots

Figure	Component	Porosity	Diffusion Coefficient (ft^2/day)	Half-life (days)	Decay Rate λ (/day)
19	Vinyl Chloride	0.25	0.2	N/A	N/A
20	Vinyl Chloride	0.05	0.2	N/A	N/A
22	Organic Acid	0.25	0.2	182.5	0.0037981
23	Organic Acid	0.25	0.2	365.0	0.0018990
25	Organic Acid	0.05	0.2	182.5	0.0037981
26	Organic Acid	0.05	0.2	365.0	0.0018990

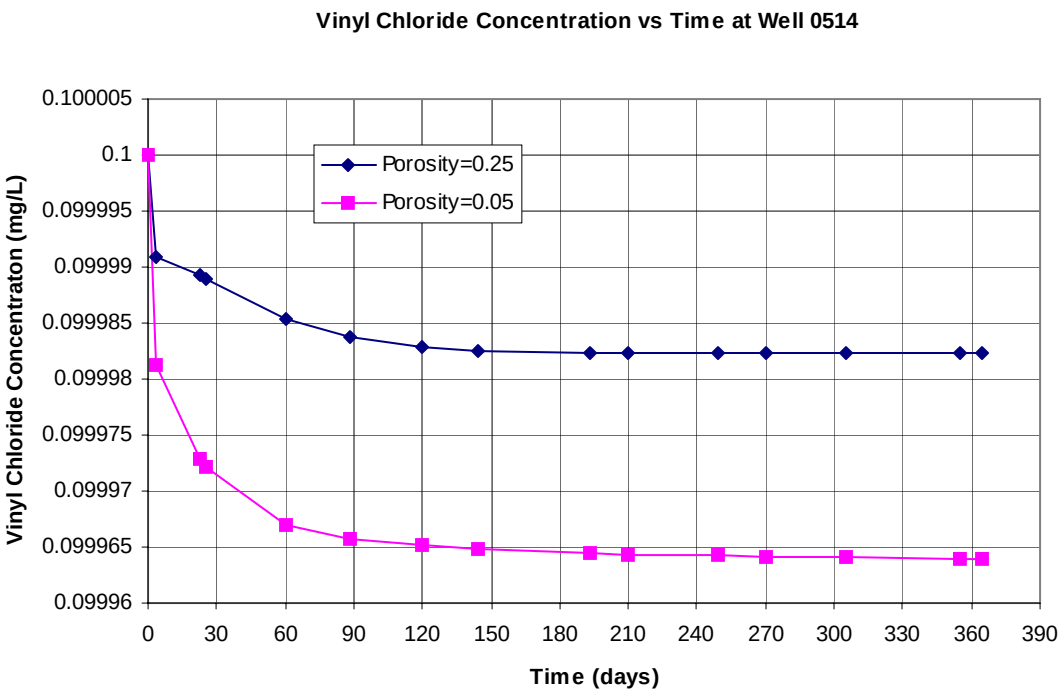

Figure 21. Vinyl Chloride Concentration versus Time at Well 0514

5.1.2 Component 2—Organic Acid

As opposed to vinyl chloride, the organic acid has an associated decay rate. Therefore, it would be expected that the concentration plumes for different parameter values would be different. Figures 22 and 23 show the distribution of the organic acid at 120 days with different parameter values as specified in Table 5. The only change is the decay rate or half-life of the organic acid. There appears to be a slight visual difference in the plots. The C1 and C2 curves in the concentration versus time plot in Figure 24 show this difference at location 0514.

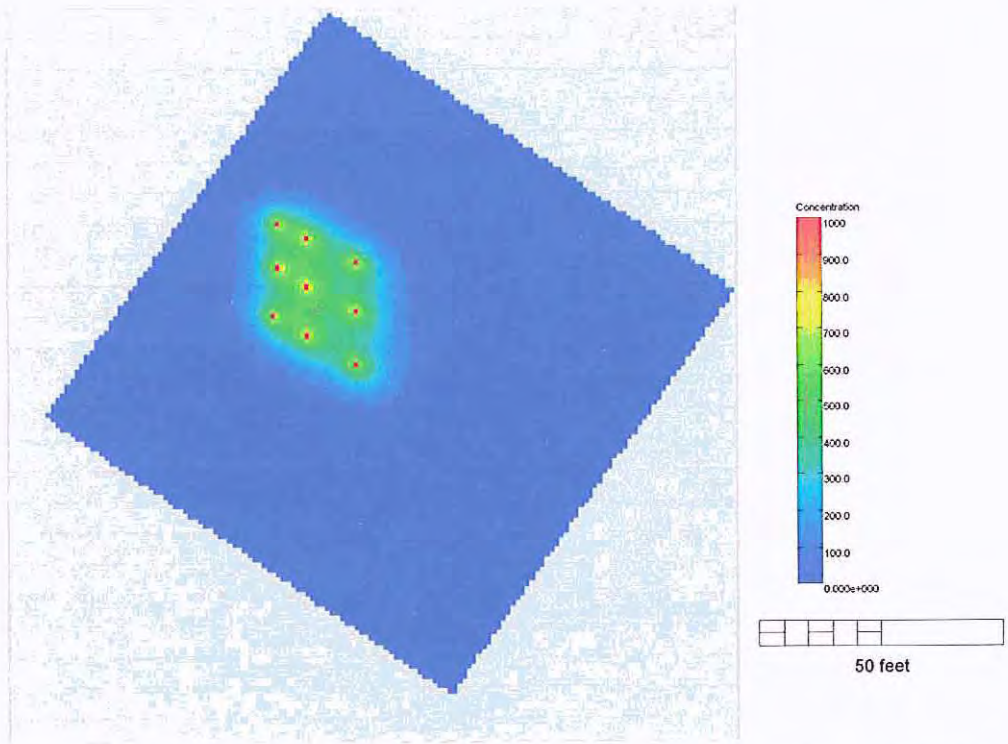

Figure 22. MT3DMS—Organic Acid (mg/L) at 120 days, Porosity=0.25, Half-life=182.5 days

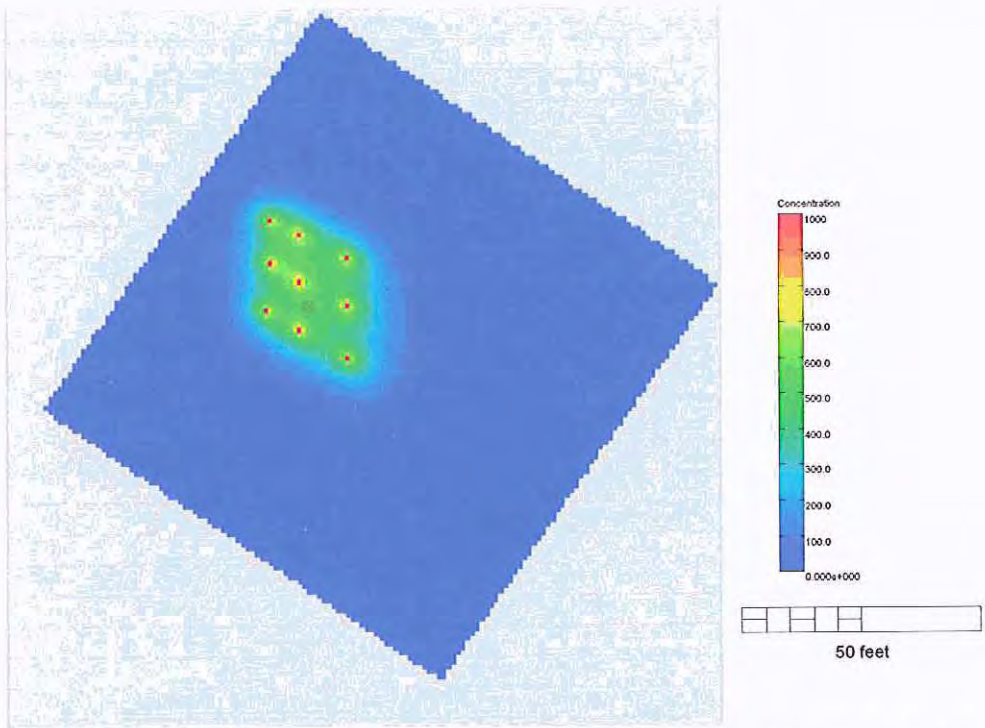

Figure 23. MT3DMS—Organic Acid (mg/L) at 120 days, Porosity=0.25, Half-life=365 days

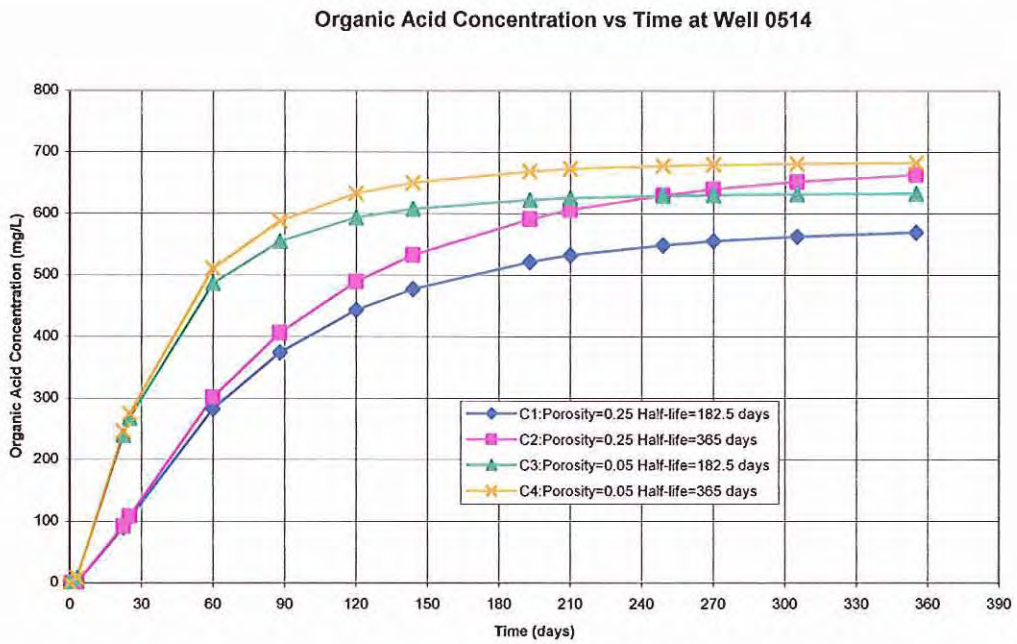

Figure 24. Organic Acid Concentration versus Time at Well 0514

Figures 25 and 26 are similar to Figures 22 and 23, respectively. The only difference in these sets of plots is the porosity (see Table 5). Figures 25 and 26 show the distribution of the organic acid at 120 days with different parameter values as shown in Table 6. The only change is the decay rate or half-life of the organic acid. Again, there appears to be a slight visual difference in the plots. The C3 and C4 curves in the concentration versus time plot in Figure 24 show this difference at location 0514.

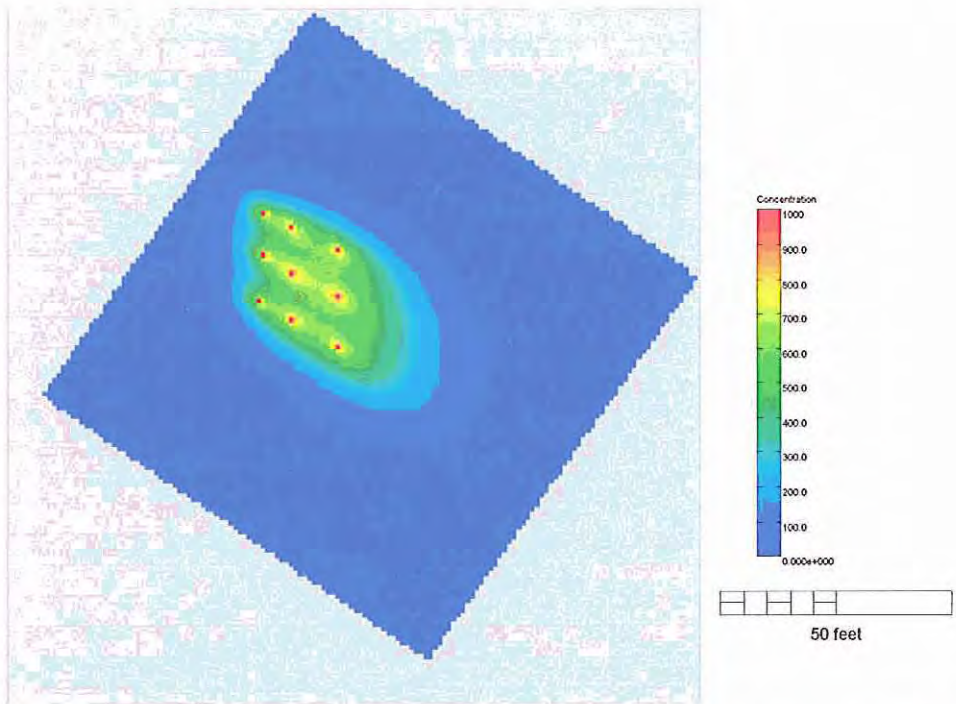

Figure 25. MT3DMS—Organic Acid (mg/L) at 120 days, Porosity=0.05, Half-life=182.5 days

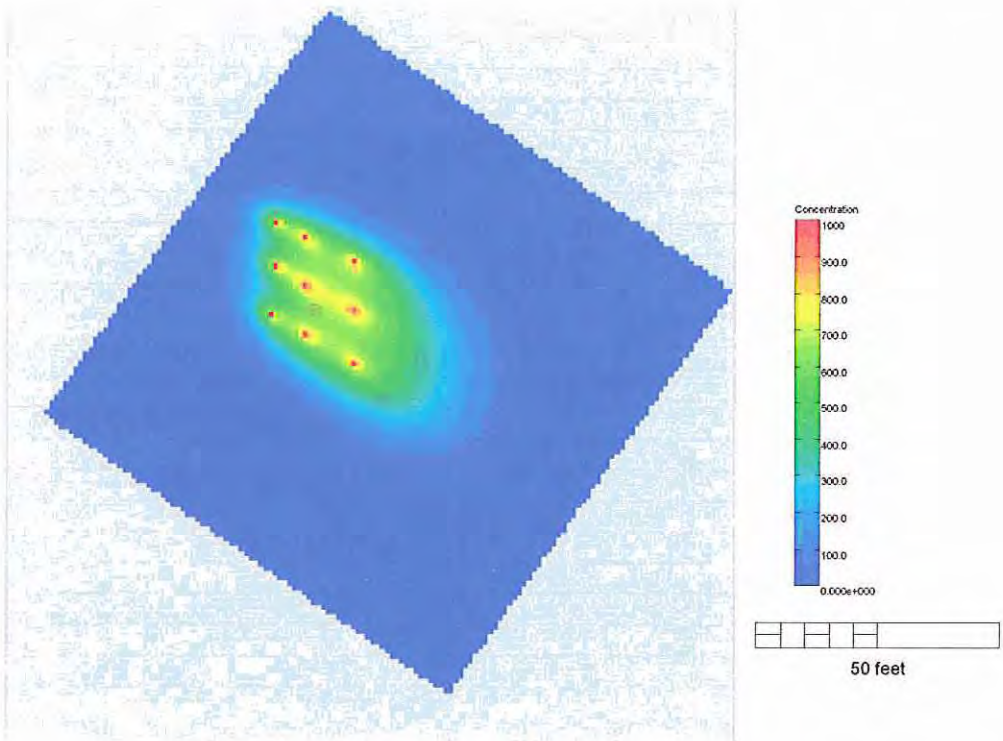

Figure 26. MT3DMS—Organic Acid (mg/L) at 120 days, Porosity=0.05, Half-life=365 days

5.1.3 Porosity and Half-life Sensitivity

In Figure 24, the curves pairs C1-C2 or C3-C4 show how the concentration changes with porosity held constant while the half-life of the organic acid varies.

The curves pairs C1-C3 or C2-C4 show how the concentration changes with the half-life of the organic acid held constant while porosity varies.

The results in Table 6 show the percent change in concentration at 120 days. The percent change is less than 10 percent if porosity is held constant and the decay rate varies. However, the percent change is greater than 25 percent if the decay rate is held constant and porosity varies.

Table 6. Porosity and Half-life Sensitivity at 120 Days

Curves	Porosity	Half-life (days)	Percent Change in Concentration
C1-C2	0.25	182.5 – 365.0	9.96
C3-C4	0.05	182.5 – 365.0	6.50
C1-C3	0.25 – 0.05	182.5	29.02
C2-C4	0.25 – 0.05	365.0	25.62

5.2 Diffusion Coefficient = 0.002 ft^2/day

This section of the analysis is similar to Part 1 except that a diffusion coefficient of 0.002 ft^2/day was used. This is closer to the upper limit of published literature values and two orders of magnitude smaller than the vendor claimed value of 0.2 ft^2/day.

5.2.1 Component 1—Vinyl Chloride

Figures 27 and 28 show the concentration plume of vinyl chloride at 120 days with different parameter values as shown in Table 7. Despite the parameter differences these figures appear to be identical. The concentration versus time plot in Figure 29 shows a slight difference at location 0514. In general, all the concentration plots of vinyl chloride at 120 days looked to be identical regardless of how porosity and the half-life values vary. This is to be expected because there is no reaction between the two components (vinyl chloride and the organic acid) and there is not a decay rate associated with vinyl chloride.

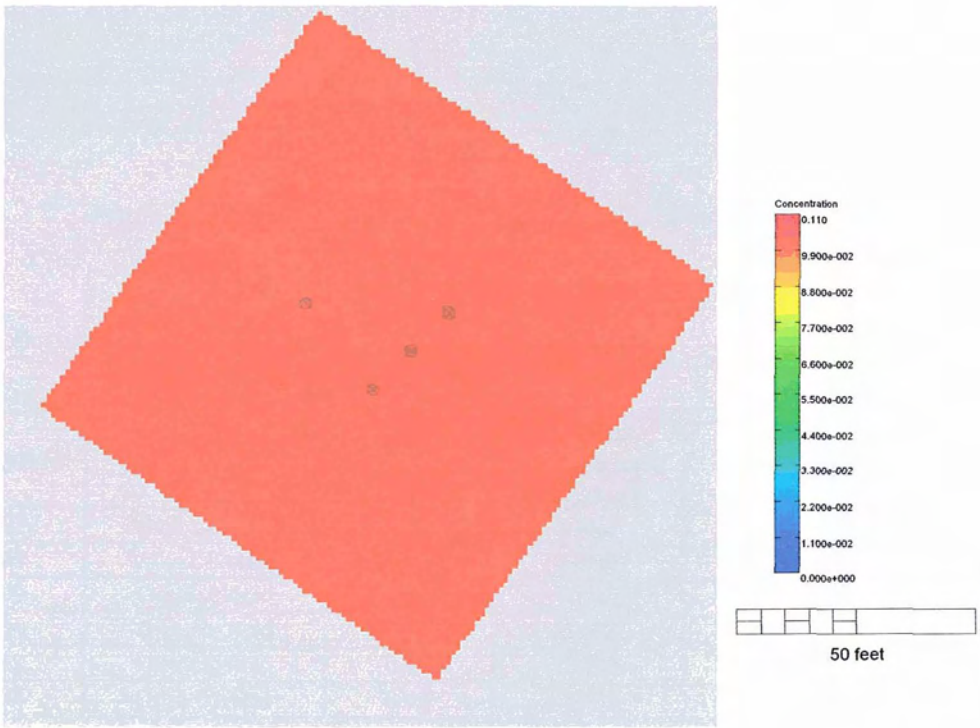

Figure 27. MT3DMS—Vinyl Chloride (mg/L) at 120 days, Porosity=0.25

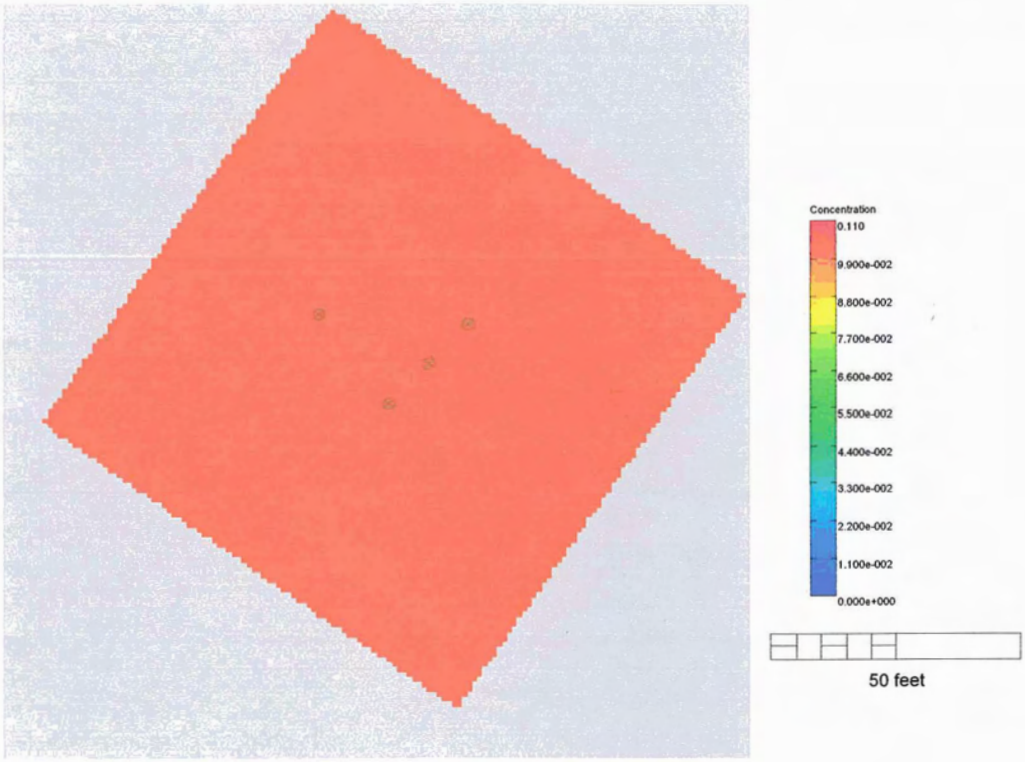

Figure 28. MT3DMS—Vinyl Chloride (mg/L) at 120 days, Porosity=0.05

Table 7. Parameter Values for Concentration Plume Plots

Figure	Component	Porosity	Diffusion Coefficient (ft^2/day)	Half-life (days)	Decay Rate λ (/day)
27	Vinyl Chloride	0.25	0.002	N/A	N/A
28	Vinyl Chloride	0.05	0.002	N/A	N/A
30	Organic Acid	0.25	0.002	182.5	0.0037981
31	Organic Acid	0.25	0.002	365.0	0.0018990
33	Organic Acid	0.05	0.002	182.5	0.0037981
34	Organic Acid	0.05	0.002	365.0	0.0018990

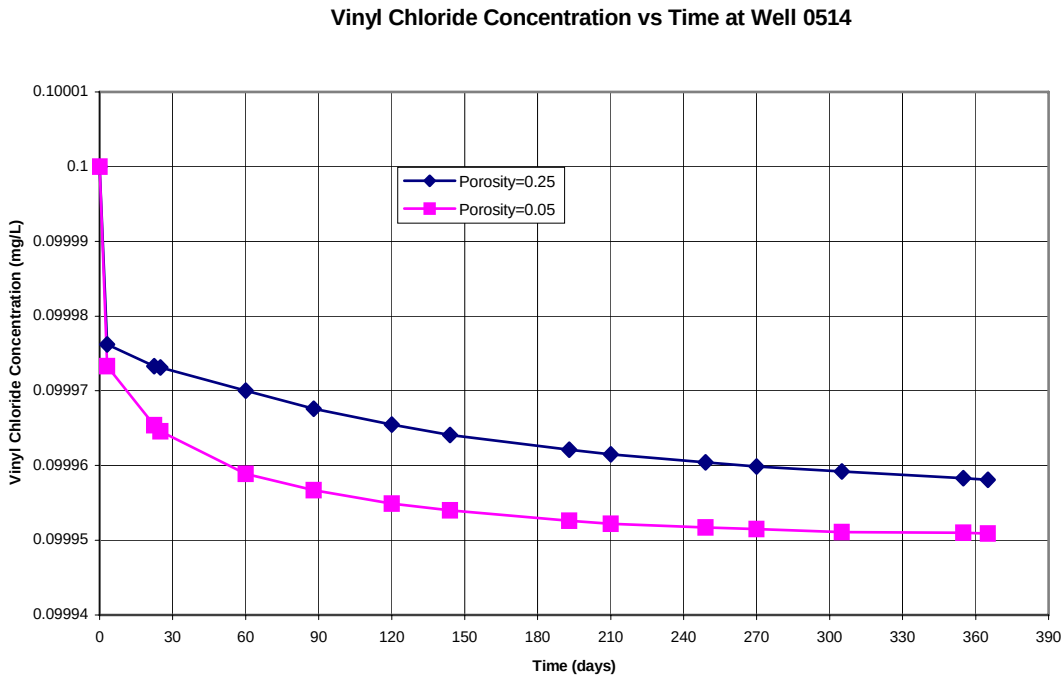

Figure 29. Vinyl Chloride Concentration versus Time at Well 0514

5.2.2 Component 2—Organic Acid

As opposed to vinyl chloride, the organic acid has an associated decay rate. Therefore, it would be expected that the concentration plumes for different parameter values would be different. Figures 30 and 31 show the distribution of the organic acid at 120 days with different parameter values as specified in Table 7. The only change is the decay rate or half-life of the organic acid. There appears to be a slight visual difference in the plots. The C1 and C2 curves in the concentration versus time plot in Figure 32 show this difference at location 0514.

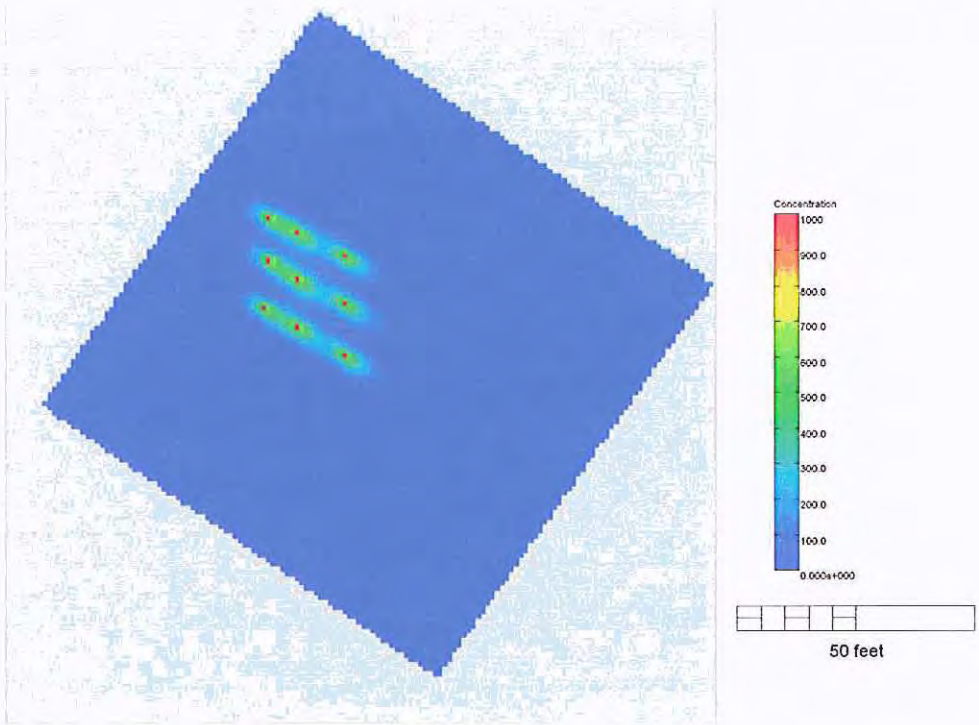

Figure 30. MT3DMS—Organic Acid (mg/L) at 120 days, Porosity=0.25, Half-life=182.5 days

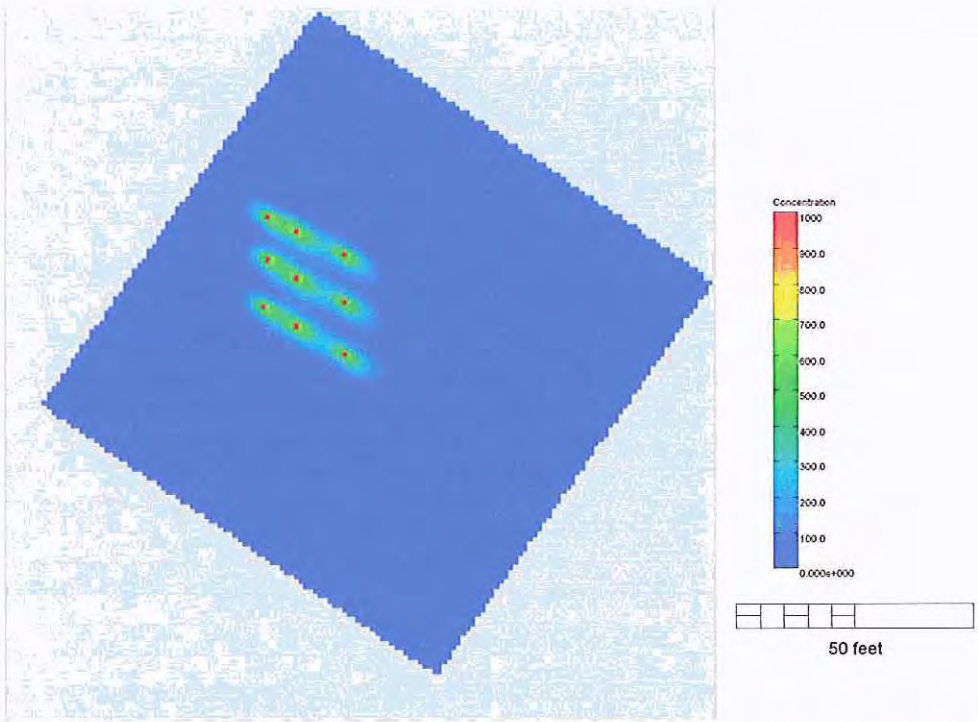

Figure 31. MT3DMS—Organic Acid (mg/L) at 120 days, Porosity=0.25, Half-life=365 days

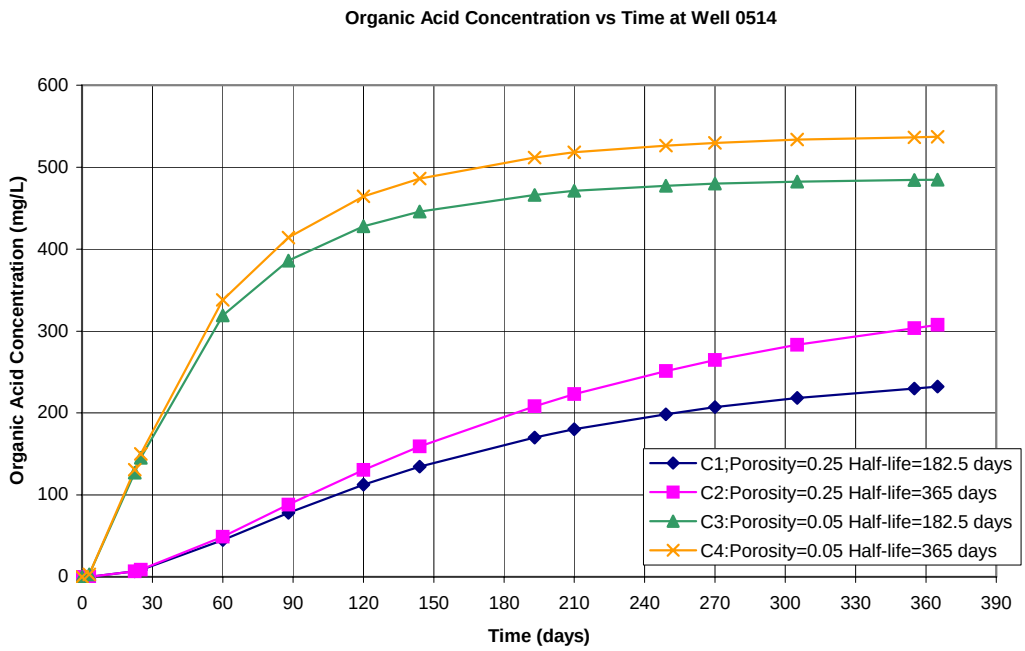

Figure 32. Organic Acid Concentration versus Time at Well 0514

Figures 33 and 34 are similar to Figures 30 and 31, respectively. The only difference in these sets of plots is the porosity (see Table 7). Figures 33 and 34 show the distribution of the organic acid at 120 days with different parameter values as shown in Table 7. The only change is the decay rate or half-life of the organic acid. Again, there appears to be a slight visual difference in the plots. The C3 and C4 curves in the concentration versus time plot in Figure 32 show this difference at location 0514.

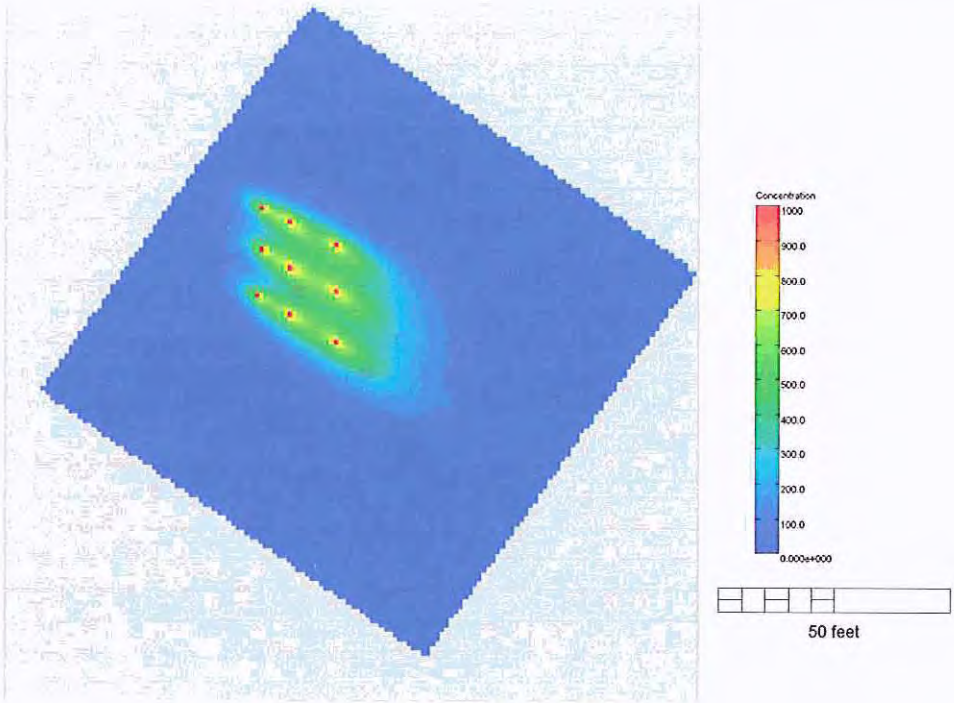

Figure 33. MT3DMS—Organic Acid (mg/L) at 120 days, Porosity=0.05, Half-life=182.5 days

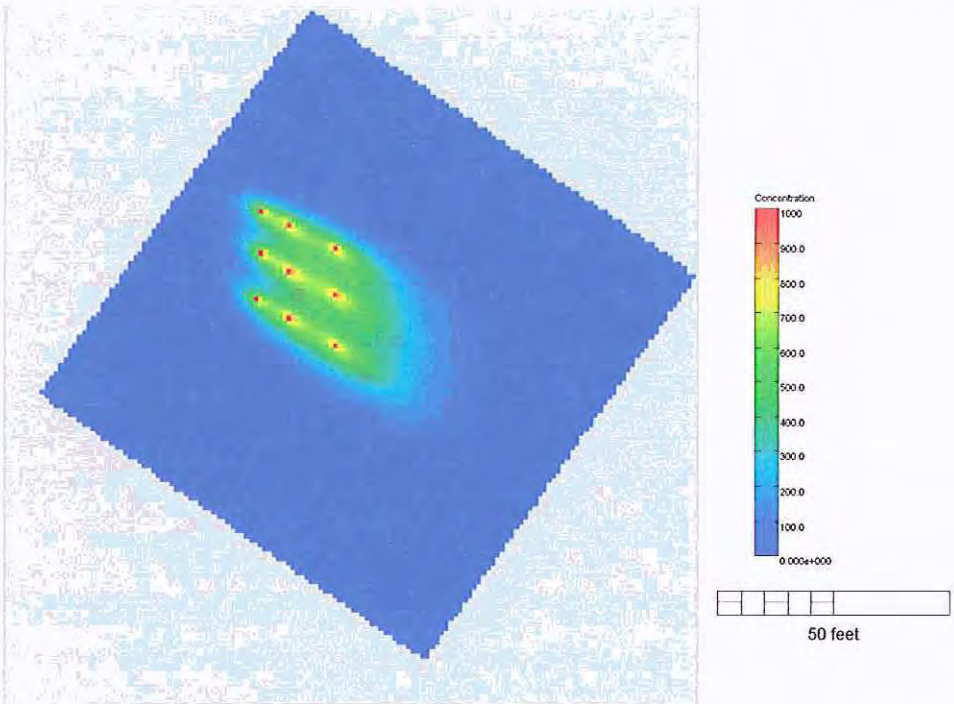

Figure 34. MT3DMS—Organic Acid (mg/L) at 120 days, Porosity=0.05, Half-life=365 days

5.2.3 Porosity and Half-life Sensitivity

In Figure 32, the curves pairs C1-C2 or C3-C4 show how the concentration changes with porosity held constant while the half-life of the organic acid varies.

The curves pairs C1-C3 or C2-C4 show how the concentration changes with the half-life of the organic acid held constant while porosity varies.

The results in Table 8 show the percent change in concentration at 120 days. The percent change is 8−15 percent if porosity is held constant and the decay rate varies. However, the percent change is greater than 100 percent if the decay rate is held constant and the porosity varies.

Table 8. Porosity and Half-life Sensitivity at 120 Days

Curves	Porosity	Half-life (days)	Percent Change in Concentration
C1-C2	0.25	182.5 – 365.0	14.96
C3-C4	0.05	182.5 – 365.0	8.19
C1-C3	0.25 – 0.05	182.5	116.79
C2-C4	0.25 – 0.05	365.0	112.21

5.3 Diffusion Coefficient Sensitivity

Table 9 displays the parameter values for the four concentration versus time plot curves in Figure 35. The results in Table 10 show the percent change in concentration at 120 days is greater than 30 percent if porosity and the decay rate are held constant and the diffusion coefficient varies.

Table 9. Parameter Values for Diffusion Coefficient Curves

Curve	Porosity	Diffusion Coefficient (ft^2/day)	Half-life (days)	Decay Rate λ (/day)
C1	0.05	0.2	182.5	0.0037981
C2	0.05	0.002	182.5	0.0037981
C3	0.05	0.2	365.0	0.0018990
C4	0.05	0.002	365.0	0.0018990

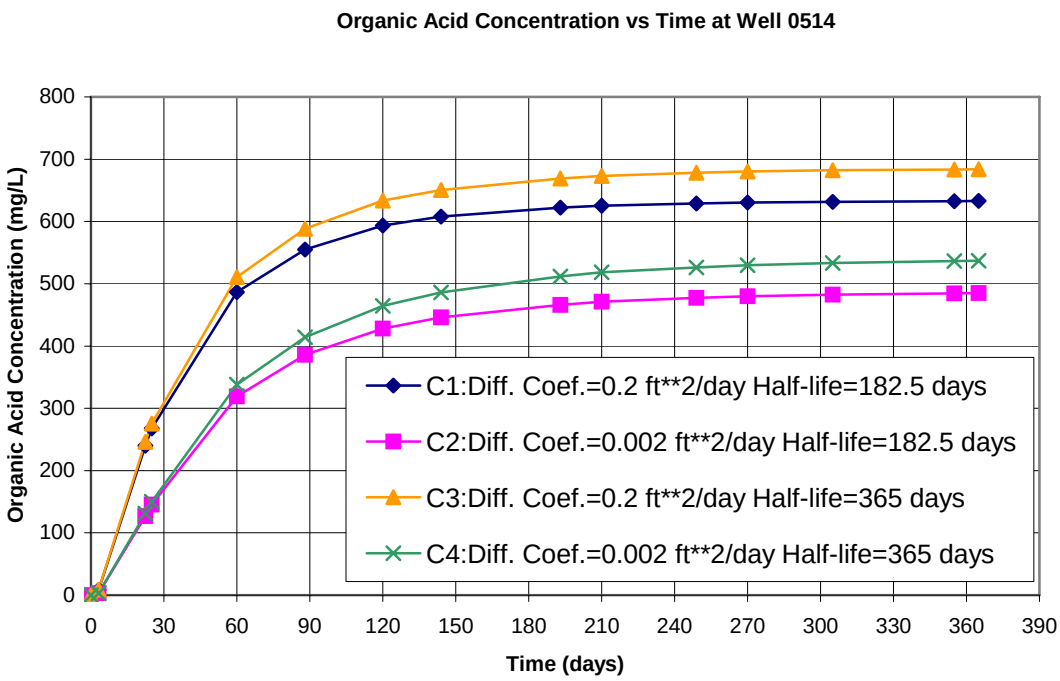

Figure 35. Organic Acid Concentration versus Time at Well 0514

Table 10. Diffusion Coefficient Sensitivity at 120 Days

Curves	Diffusion Coefficient (ft^2/day)	Porosity	Half-life (days)	Percent Change in Concentration
C1-C2	0.2 – 0.002	0.05	182.5	32.40
C3-C4	0.2 – 0.002	0.05	365.0	30.75

5.4 MT3DMS Model Conclusions

The sensitivity analysis indicates that porosity is the most sensitive of the three parameters in this MT3DMS model. This is particularly evident at a diffusion coefficient value of 0.002 ft^2/day (see Table 8). The percent change in concentration is greater than 100% between the two porosity values. Therefore, it would be important to determine site-specific porosity values and whether preferred flow paths exist. The justification for low porosity values is discussed in Appendix A.

The diffusion coefficient is the next most sensitive of the three parameters. The percent change in concentration is approximately 31 percent between the two diffusion coefficient values (see Table 10). This is very close to the values determined in the barrier wall design of Section 4.3 and the value reported in Section 4.4.

The decay rate or half-life associated with the organic acid is the least sensitive. Although not as sensitive as the other parameters the percent change in concentration is still in the range of 10−15 percent with a diffusion coefficient of 0.002 ft^2/day. This is an indication that the

approach of using one decay rate to account for all the hydrogen electron reductive reactions that must occur before or simultaneously with the reductive dechlorination does not adequately model the process. This approach assumed that all the other hydrogen electron reductive reactions are taken care of before any reductive dechlorination occurs, when in fact the reactions are not mutually exclusive and several may occur simultaneously. A more complex model is needed to account for these reactions.

6.0 RT3D Modeling

The MT3DMS multi-species two-component concentration results for vinyl chloride and the organic acid at 120 days were used as initial concentrations in an RT3D instantaneous model. This time of 120 days is the assumed lag time before vinyl chloride degradation begins. The MT3DMS results used to produce the initial concentration input to the RT3D model are shown in Table 11.

Table 11. MT3DMS Parameters

Parameter	Value
Porosity	0.05
Half-life (days)	182.5
Decay Rate λ (/day)	0.0037981
Diffusion Coefficient (ft^2/day)	0.002

RT3D has seven preprogrammed reaction modules. Model #1, a 2-component instantaneous reaction model, is used to model the reductive declorination of vinyl chloride by a microbially-mediated organic acid. Instantaneous reaction between any two chemicals can be simulated by changing the stoichiometric ratio F. In this reaction model, BTEX (component 1) is replaced by vinyl chloride and oxygen (component 2) is replaced by the organic acid. The stoichiometric ratio of the organic acid to the sum of the electron demands (such as nitrate, sulfate, iron, as well as contaminants such as vinyl chloride) is not known. Therefore for demonstration purposes two estimated values will be used.

The reader is reminded that the RT3D predictions presented in the following sections regarding the removal of vinyl chloride via reductive dechlorination are somewhat optimistic because they are based on the assumed presence of preferred flow paths. Accordingly, it is important to recognize that the predicted efficacy of contaminant reduction applies to vinyl chloride in the preferred flow paths, but may not represent vinyl chloride in the less permeable zones between preferred paths.

6.1 Stoichiometric Ratio F = 10

Vinyl chloride concentration at 0 days is shown in Figure 28 of Section 5.2.1. Organic acid concentration at 0 days is shown in Figure 33 of Section 5.2.2. In Figures 36 through 41 the stoichiometric ratio F = 10. Figures 36, 37, and 38 show vinyl chloride at 25 days, 88 days, and 365 days, respectively. Figures 39, 40, and 41 show the organic acid at 25 days, 88 days, and 365 days, respectively.

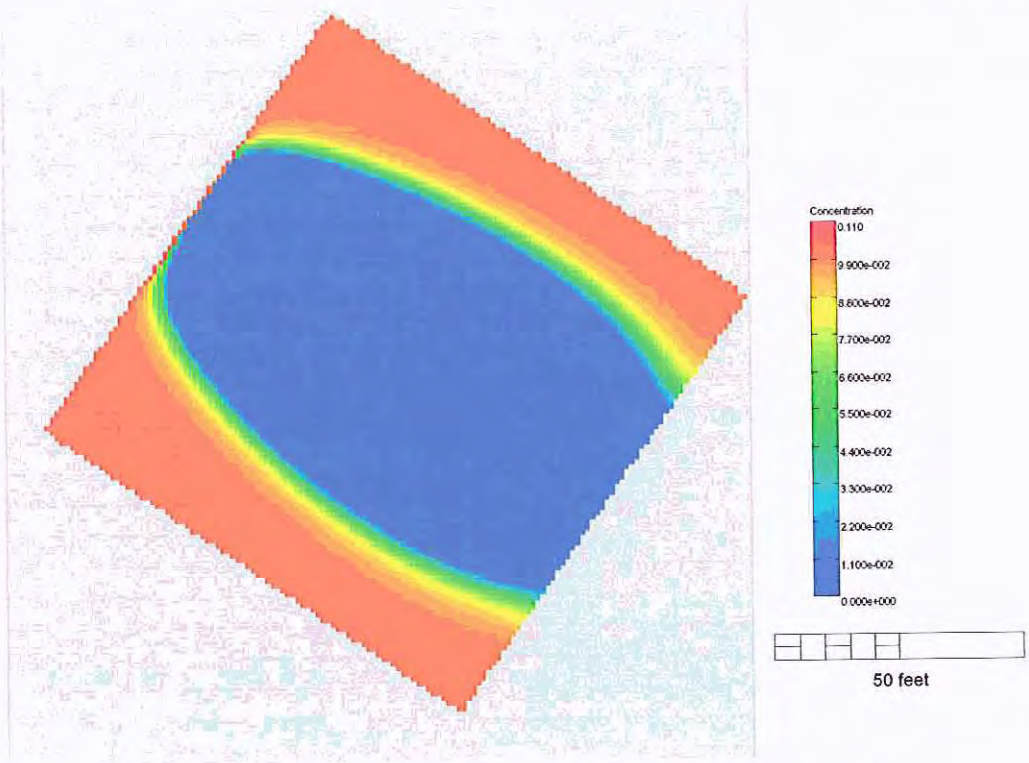

Figure 36. RT3D—Vinyl Chloride (mg/L) at 25 days F=10

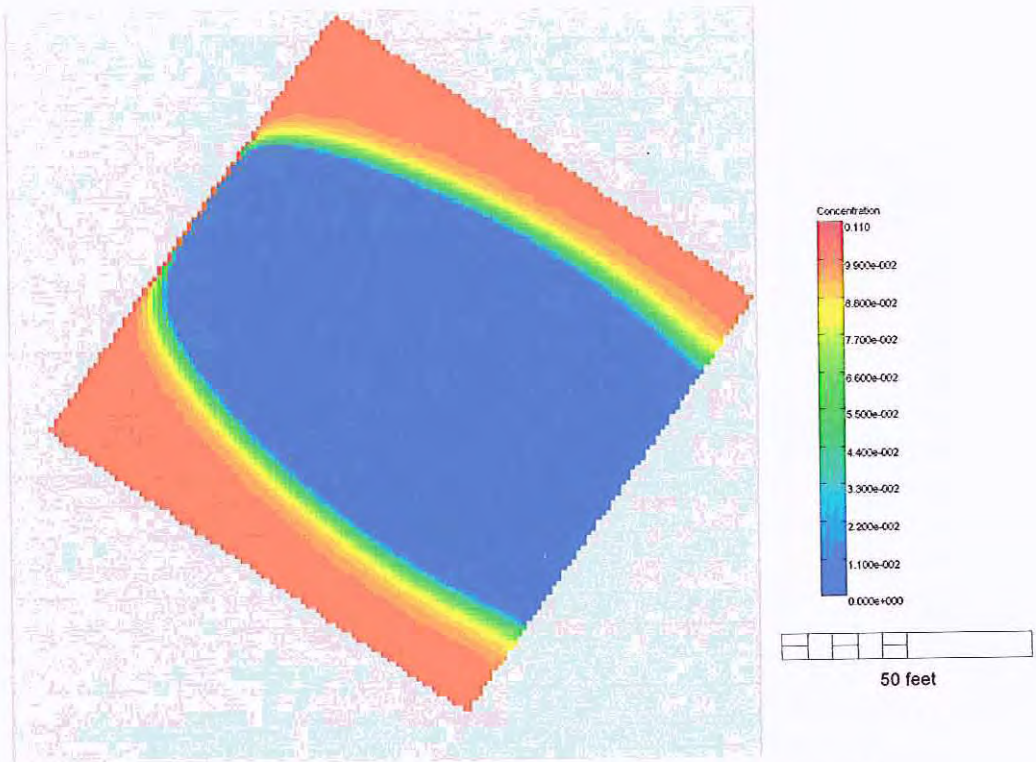

Figure 37. RT3D—Vinyl Chloride (mg/L) at 88 days F=10

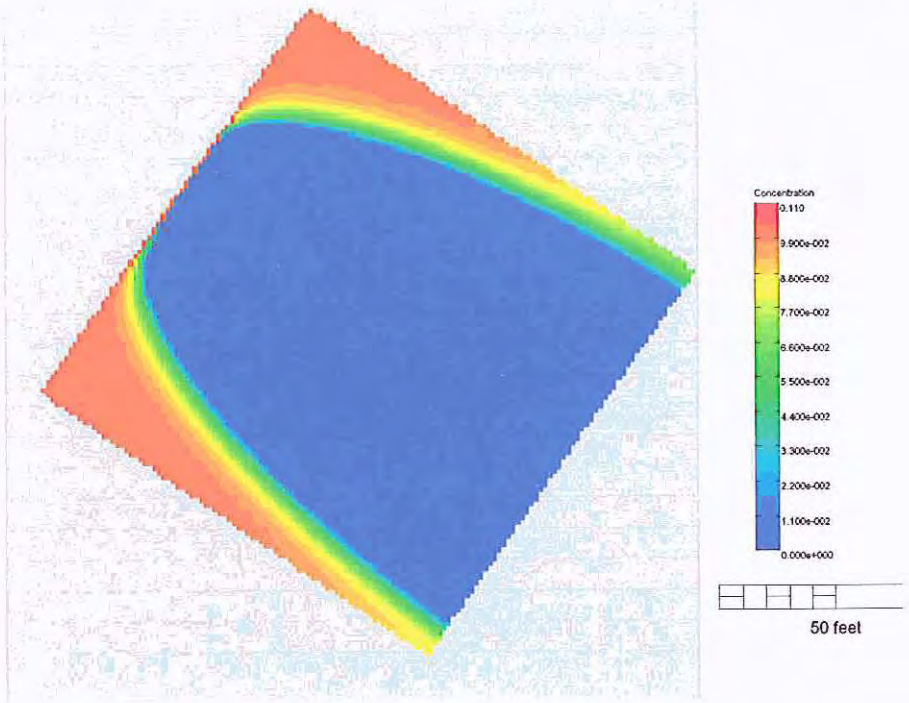

Figure 38. RT3D—Vinyl Chloride (mg/L) at 365 days F=10

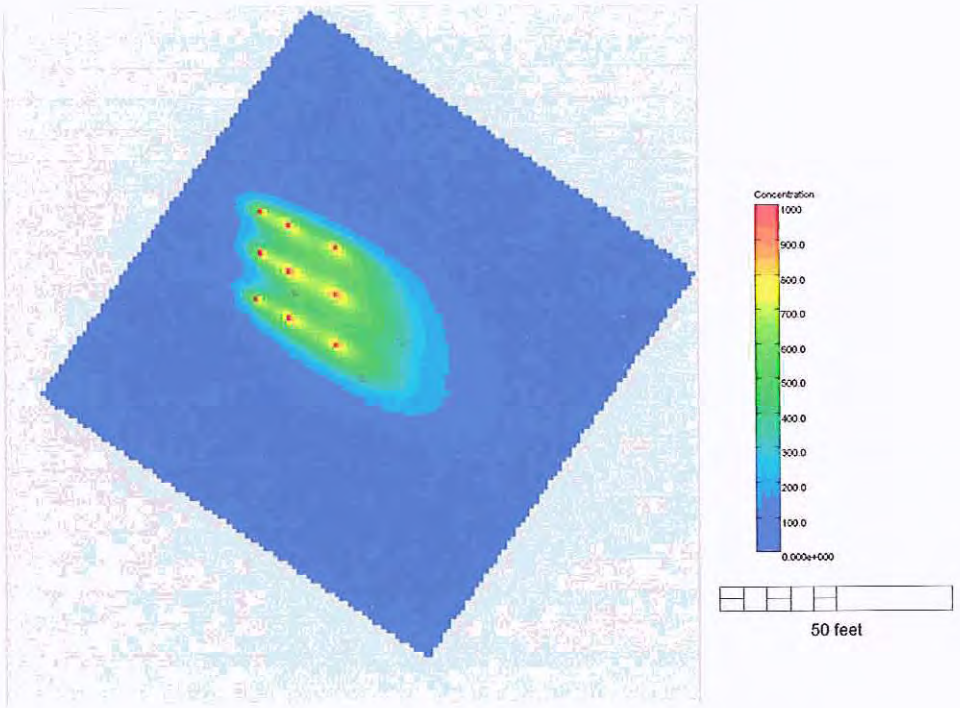

Figure 39. RT3D—Organic Acid (mg/L) at 25 days F=10

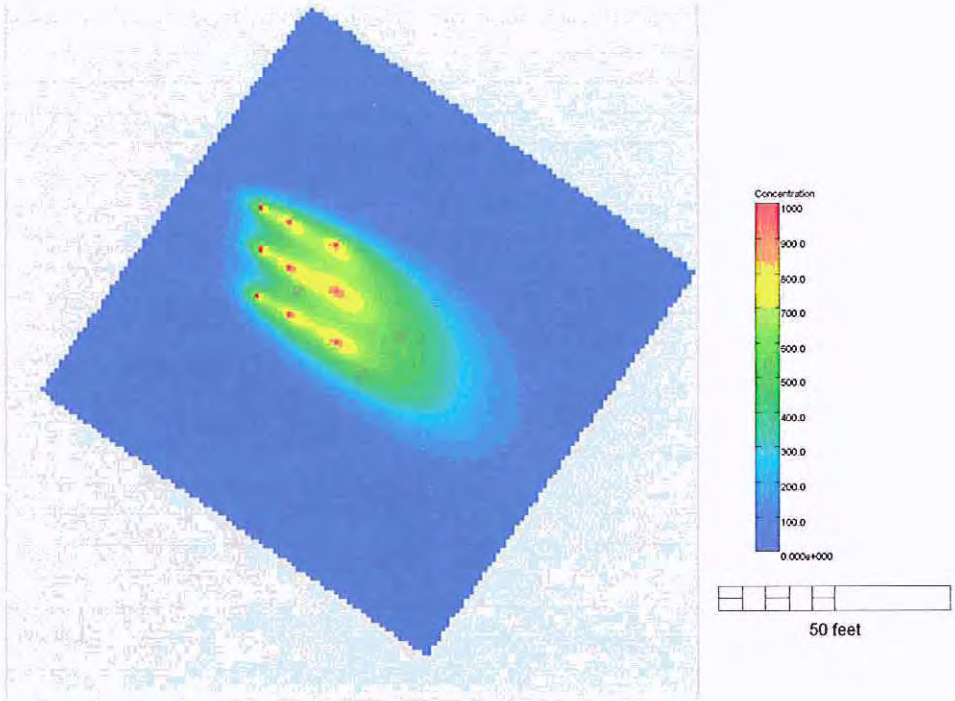

Figure 40. RT3D—Organic Acid (mg/L) at 88 days F=10

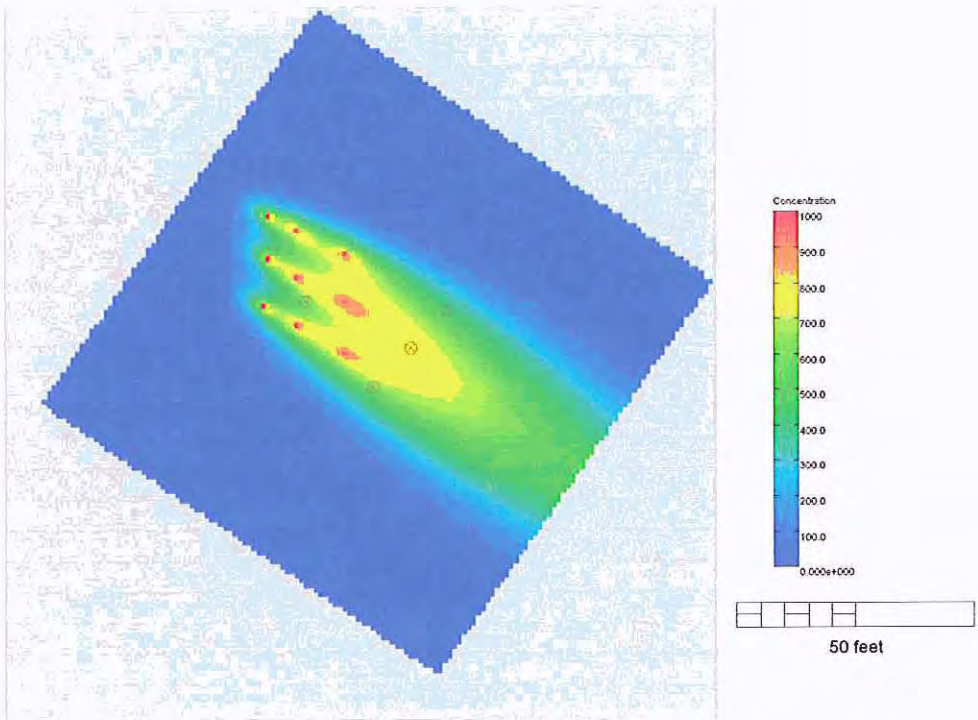

Figure 41. RT3D—Organic Acid (mg/L) at 365 days F=10

6.2 Stoichiometric Ratio F = 10000

In Figures 42 through 47 the stoichiometric ratio F = 10000. Figures 42, 43, and 44 show vinyl chloride at 25 days, 88 days, and 365 days, respectively. Figures 45, 46, and 47 show the organic acid at 25 days, 88 days, and 365 days, respectively.

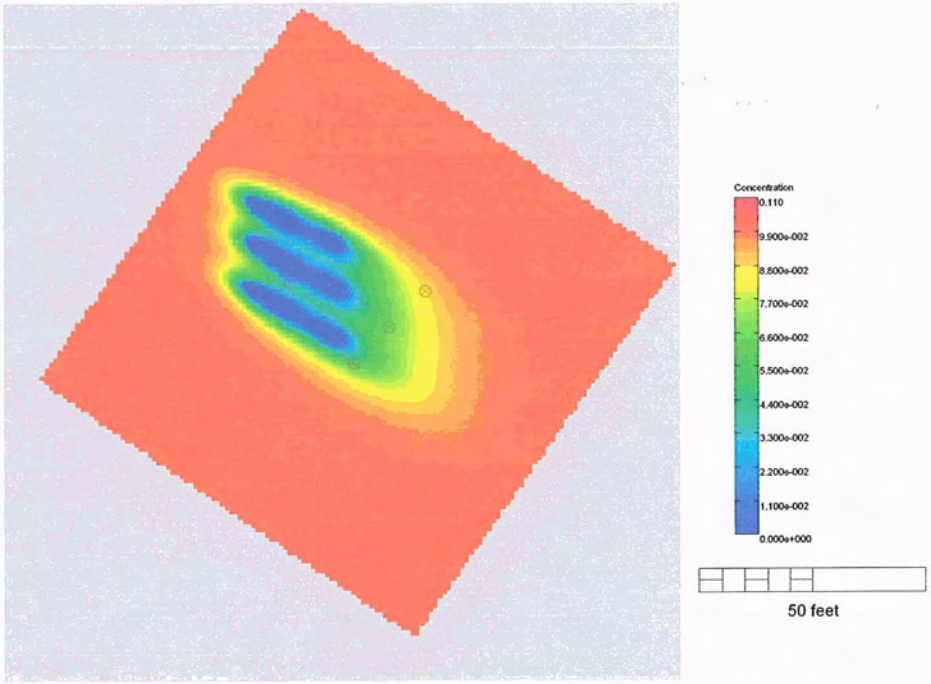

Figure 42. RT3D—Vinyl Chloride (mg/L) at 25 days F=10000

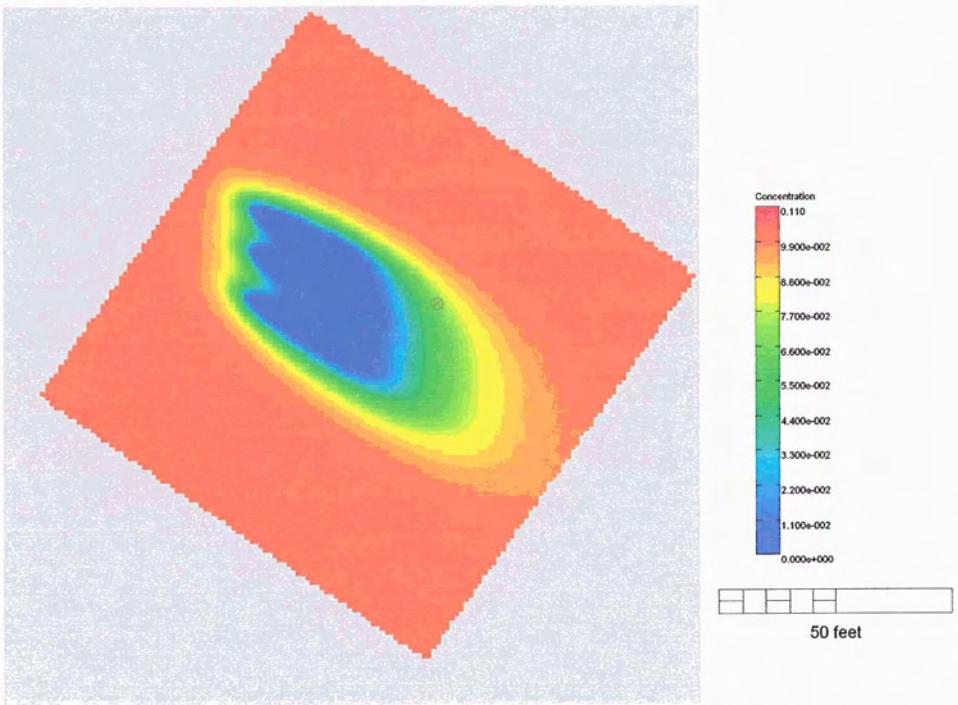

Figure 43. RT3D—Vinyl Chloride (mg/L) at 88 days F=10000

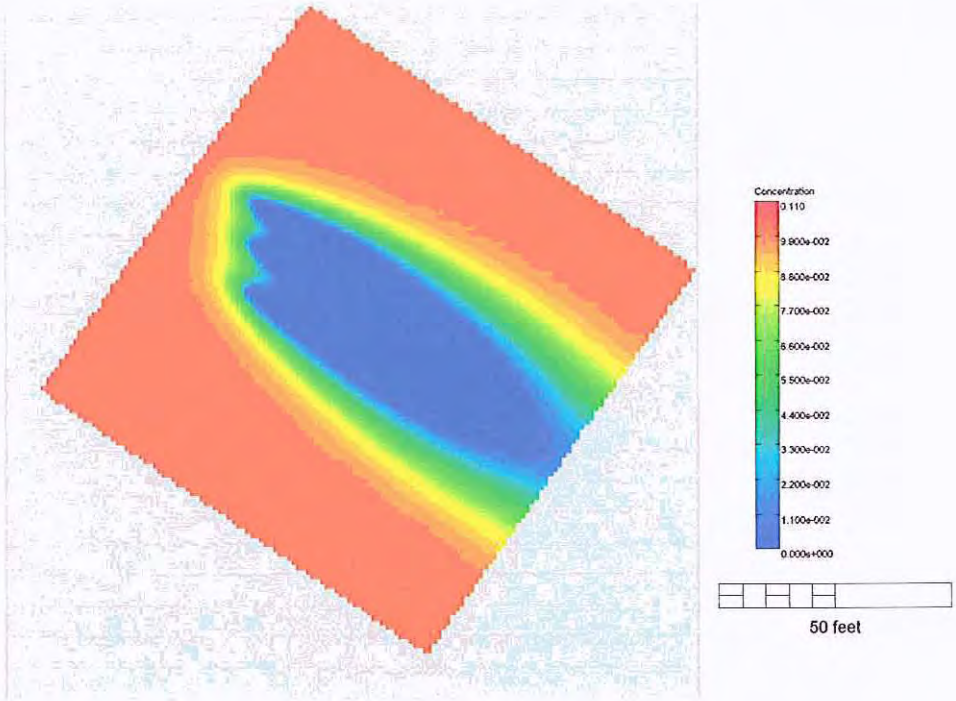

Figure 44. RT3D—Vinyl Chloride (mg/L) at 365 days F=10000

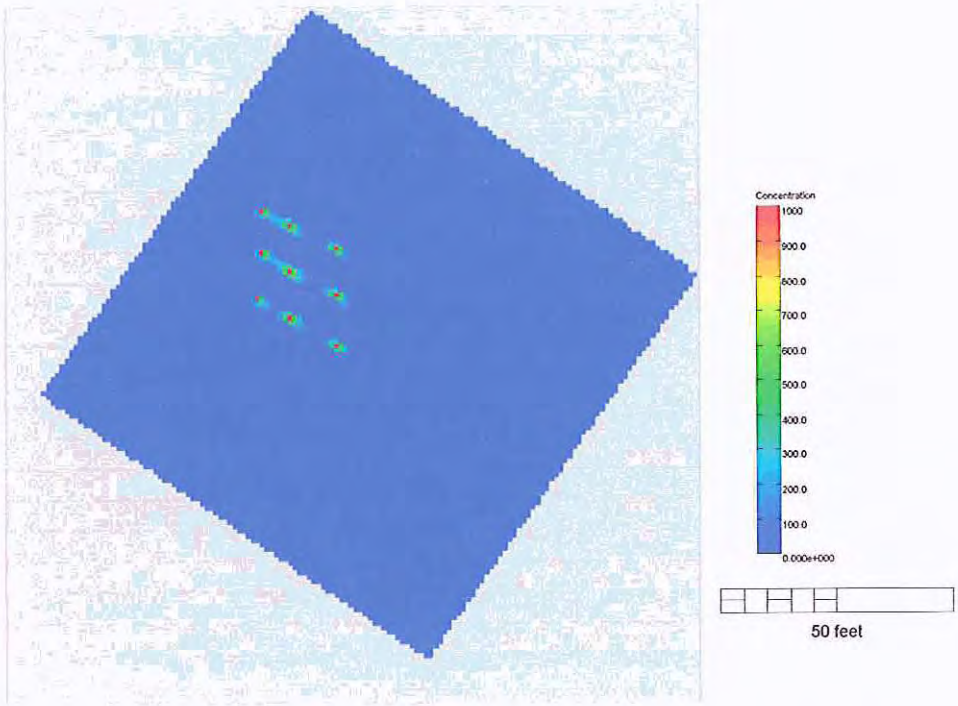

Figure 45. RT3D—Organic Acid (mg/L) at 25 days F=10000

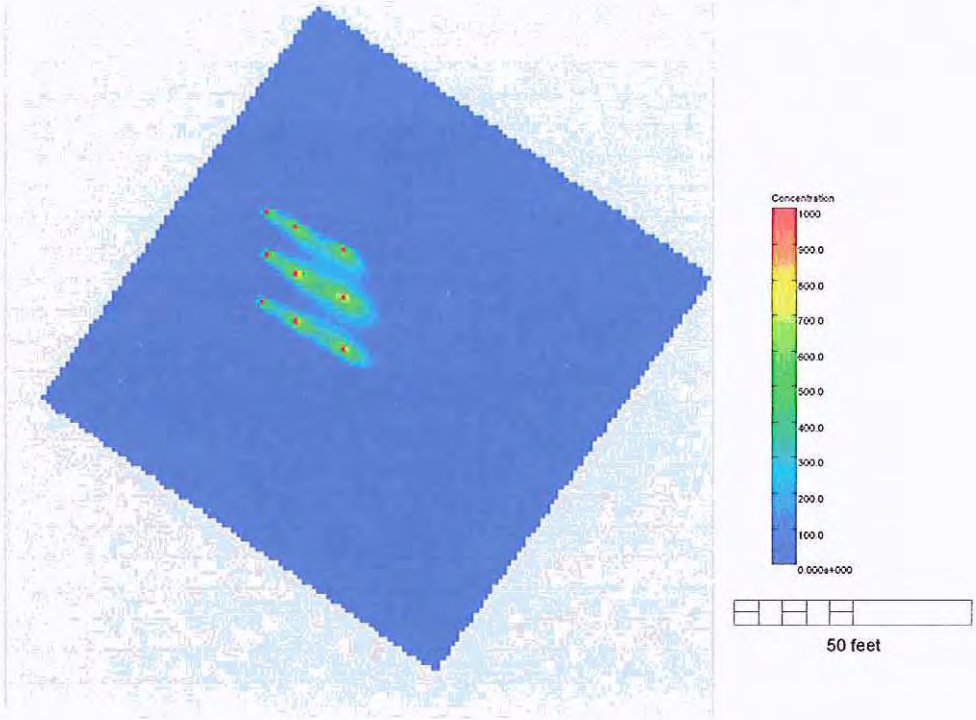

Figure 46. RT3D—Organic Acid (mg/L) at 88 days F=10000

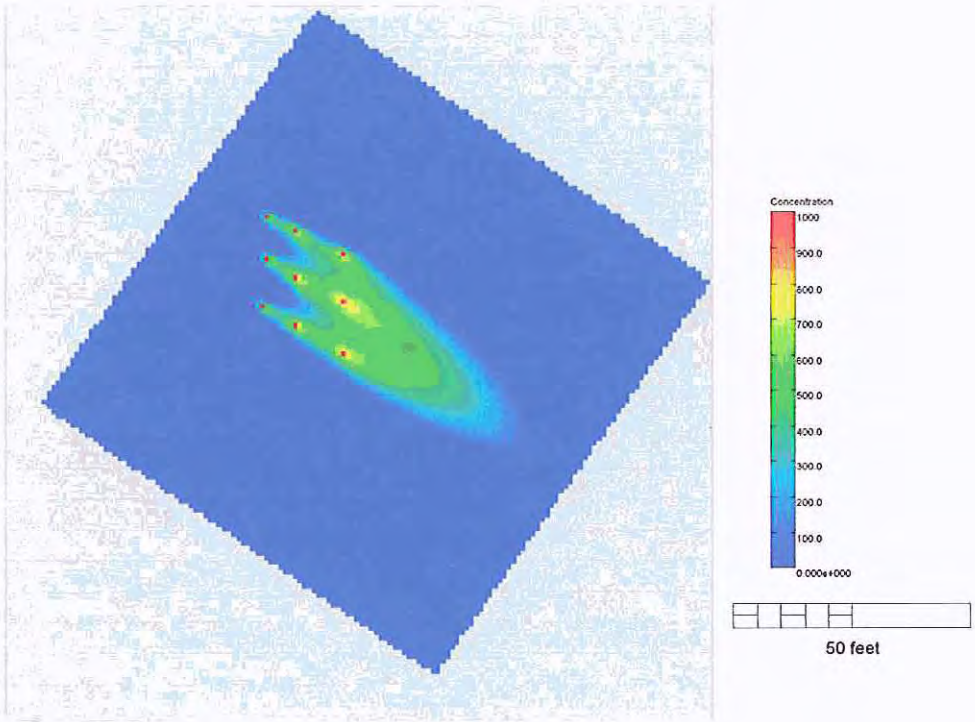

Figure 47. RT3D—Organic Acid (mg/L) at 365 days F=10000

6.3 Stoichiometric Ratio Sensitivity

Figure 48 shows the organic acid concentration versus time plots for the two stoichiometric ratios at two locations. From Figures 41, 47, and 48 and Table 12 it is apparent that the organic acid concentration changes significantly with this magnitude of change in the stoichiometric ratio.

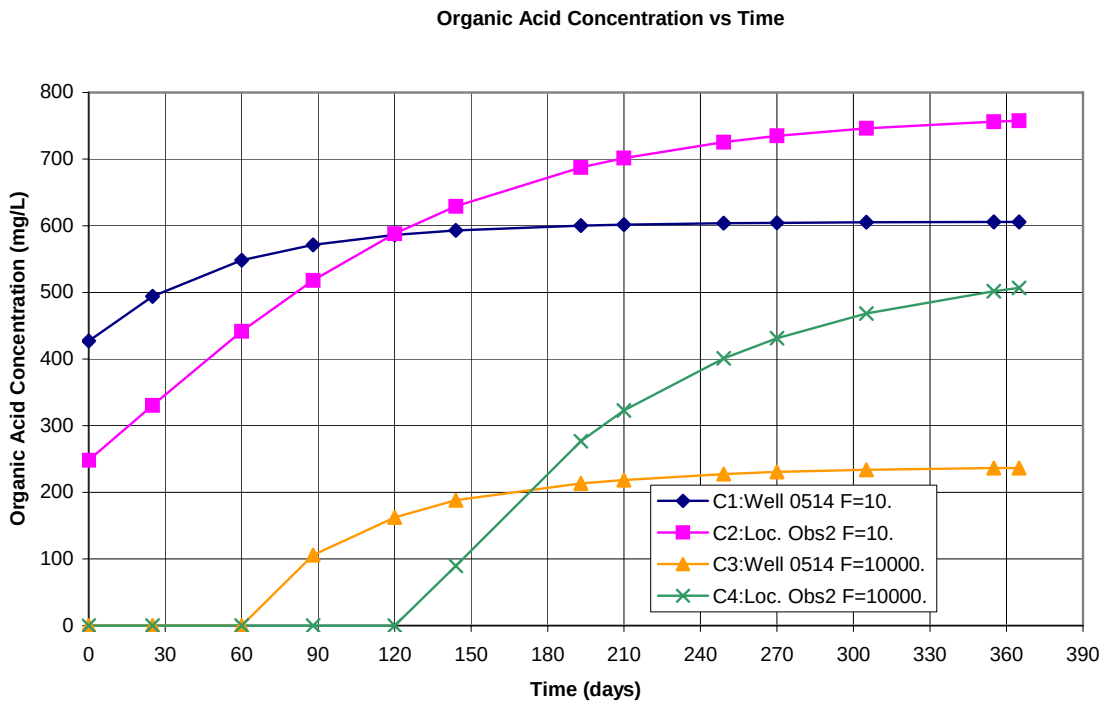

Figure 48. Organic Acid Concentration versus Time

Table 12. Stoichiometric Ratio Sensitivity at 365 Days

Curves	Stoichiometric Ratios	% Change in Concentration
C1-C3	10. – 10000.	87.66
C2-C4	10. – 10000.	39.70

6.4 RT3D Model Conclusions

The results of this RT3D instantaneous reaction model show that it is very sensitive to the stoichiometric ratio. This further suggest that this approach of attempting to use a single stoichiometric value falls significantly short of accounting for all the electron demand reactions that must be satisfied before reductive dechlorination occurs.

7.0 Summary and Conclusions

The model presented here successfully simulates HRC penetration and lactic acid migration and determines the sensitivity of diffusion coefficients, aquifer porosity, and organic acid decay rates. The model also accommodates reductive dechlorination of chlorinated solvents in a rudimentary fashion, but the large number of significant assumptions that must be made brings into question the validity of the simulation. The uncertainties in the possible presence of preferred flow paths and associated effective porosity, the diffusion coefficients of HRC and the resulting acids, and the combination of the numerous non-contaminant electron demands into one stoichiometric ratio strongly emphasize the shortcomings of the technical approach.

Because of these shortcomings and software limitations, Stoller conducted research to determine other options for modeling software and to assess the feasibility of custom development of the RT3D modeling software. Discussions with Regenesis, the company that makes HRC, indicated that only one other group of workers had attempted a similar model. Unfortunately, Regenesis was unable to provide Stoller with contact information for the other workers. Subsequently, Stoller contacted researchers at Battelle Pacific Northwest Division, the authors of the RT3D modules. They indicated that they also had realized these same limitations and had started working toward a solution. They offered to produce a customized RT3D simulation module that would solve most or all of the problems associated with the current model. As far as Stoller can determine, this is the only option for solving the modeling issues.

A customized RT3D model that accurately simulated bioremediation would answer many of the questions raised by this model. Some advantages are:

- The model will be able to account for the other electron acceptors individually. Rather than lumping nitrate, manganese, iron, sulfate, etc., as a group of electron acceptors, each component can be accounted for individually as they occur in nature. This will allow for a much more realistic simulation of exactly when individual contaminants will begin to degrade and when the degradation will be complete.
- In the current baseline, enhanced bioremediation is the preferred final cleanup strategy at the Northeast Site, the Building 100 Area, and the 4.5 Acre Site. An accurate enhanced bioremediation model using the customized RT3D reaction module can be used for these locations to predict cleanup times and produce more accurate cost estimates.
- There will be an opportunity to adjust the reaction parameters, decay rates, porosity, etc., to match the measured field concentration data.
- The model will allow a thorough understanding of results. If problems are encountered, an accurate model will greatly aid in solving the problem.
- The model will help optimize design at each individual site, avoiding costs associated with assumptions that are too conservative.
- The model may also be used to evaluate the applicability and time frame for potential long-term natural attenuation scenarios, and aid other decision making.

In summary, the cost of this custom RT3D module will be repaid many times over as enhanced bioremediation is implemented at the STAR Center.

8.0 References

Freeze, R.A., and J.A. Cherry, 1979. *Groundwater*, Prentice-Hall Inc., Englewood Cliffs, New Jersey.

Hayduk, W. and H. Laudie, 1974. "Prediction of Diffusion Coefficients for Non-electrolysis in Dilute Aqueous Solutions," *AIChEJ*, 20:611-15.

Kruseman, G.P., and N.A. de Ridder, 1991. *Analysis and Evaluation of Pumping Test Data*, Section 15.2.2, Page 230, 2nd Edition, International Institute for Land Reclamation and Improvement, P.O. Box 45, 6700 AA Wageningen, The Netherlands.

Regenesis, HRC Technical Bulletin #1.1.2, "Biological Reductive Dechlorination of CAHs."

Regenesis, HRC Technical Bulletin #2.8.2, "Distribution of HRC in the Aquifer."

Winflow2 (ESI 2000).

Appendix A

Justification for Low Porosity Analogy Between Preferred Flow Paths And Fractured Flow

Preferred flow paths can exist in unconsolidated deposits such as those that comprise the Pinellas surficial aquifer. In essence, these paths represent zones in which the hydraulic conductivity is somewhat higher than occurs in the remaining part of the aquifer. From a ground water transport perspective, the preferred flow paths in unconsolidated media are analogous to fractures in consolidated rock. That is, just as ground water will move much faster through fractures than it will through a rock matrix, so too will it move faster through a preferred path than through less permeable portions of an unconsolidated medium. To account for more rapid ground water movement through preferred flow paths, which translates into faster movement of dissolved chemicals, the relatively low porosity represented by fractures is sometimes adopted. In an analogous fashion, a porosity value lower than that associated with unconsolidated deposits can be used to estimate faster chemical movement via preferred flow paths.